

This is an Open Access document downloaded from ORCA, Cardiff University's institutional repository:<https://orca.cardiff.ac.uk/id/eprint/160851/>

This is the author's version of a work that was submitted to / accepted for publication.

Citation for final published version:

Incoom, Awo Boatemaa Manson, Adjei, Kwaku Amaning, Odai, Samuel Nii, Akpoti, Komlavi, Siabi, Ebenezer Kwadwo and Awotwi, Alfred 2023. Assessing climate model accuracy and future climate change in Ghana's Savannah regions. *Journal of Water & Climate Change* 10.2166/wcc.2023.070 file

Publishers page: <http://dx.doi.org/10.2166/wcc.2023.070>






Please note:

Changes made as a result of publishing processes such as copy-editing, formatting and page numbers may not be reflected in this version. For the definitive version of this publication, please refer to the published source. You are advised to consult the publisher's version if you wish to cite this paper.

This version is being made available in accordance with publisher policies. See <http://orca.cf.ac.uk/policies.html> for usage policies. Copyright and moral rights for publications made available in ORCA are retained by the copyright holders.



Assessing climate model accuracy and future climate change in Ghana's Savannah regions

Awo Boatemaa Manson Incoom ^{a,b,*}, Kwaku Amaning Adjei ^{a,b}, Samuel Nii Odai ^c, Komlavi Akpoti ^d, Ebenezer Kwadwo Siabi ^{e,f} and Alfred Awotwi^g

^a University of Energy and Natural Resources, Sunyani, Ghana

^b Kwame Nkrumah University of Science and Technology, Kumasi, Ghana

^c Accra Technical University, Accra, Ghana

^d International Water Management Institute (IWMI), Accra, Ghana

^e Earth Observation Research and Innovation Centre (EORIC), University of Energy and Natural Resources, P. O. Box 214, Sunyani, Ghana

^f Regional Center for Energy and Environmental Sustainability, University of Energy and Natural Resources, P.O. Box 214, Sunyani, Ghana

^g School of Earth and Environmental Sciences, Cardiff University, Cardiff, Wales

*Corresponding author. E-mail: awoboat@yahoo.co.uk; awomanson@gmail.com

 ABMI, 0000-0003-1181-4125; KAA, 0000-0003-3220-6735; SNO, 0000-0002-9910-5376; KA, 0000-0001-6435-5116; EKS, 0000-0001-8563-6689

ABSTRACT

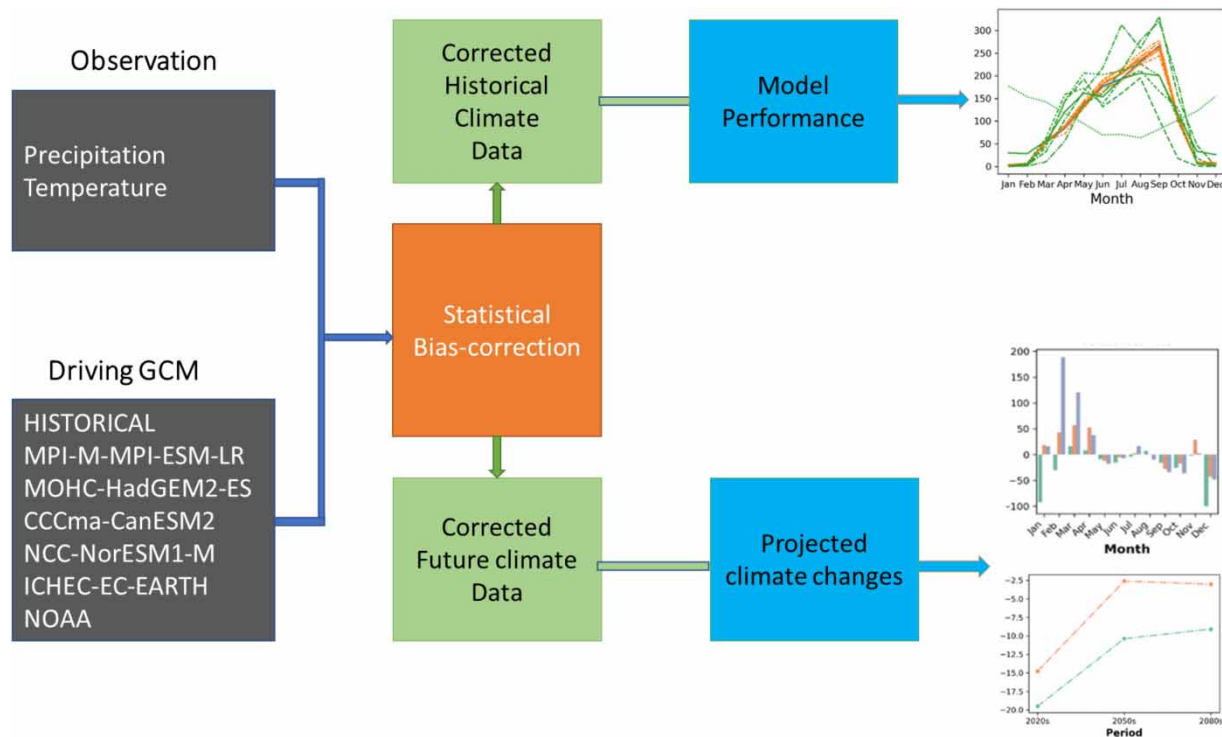
This study aimed to compare the performance of six regional climate models (RCMs) in simulating observed and projecting future climate in the Savannah zone of Ghana, in order to find suitable methods to improve the accuracy of climate models in the region. The study found that the accuracy of both individual RCMs and their ensemble mean improved with bias correction, but the performance of individual RCMs was dependent on location. The projected change in annual precipitation indicated a general decline in rainfall with variations based on the RCM and location. Projections under representative concentration pathway (RCP) 8.5 were larger than those under RCP 4.5. The mean temperature changes recorded were 1 °C for the 2020s for both RCPs, 1–4 °C for the 2050s under both RCPs, and 1–4 °C under RCP 4.5, and from 2 to 8 °C for the 2080s. These findings will aid farmers and governments in the West African subregion in making informed decisions and planning cost-effective climate adaptation strategies to reduce the impact of climate change on the ecosystem. The study highlights the importance of accurate climate projections to reduce vulnerability to climate change and the need to improve climate models in projecting climate in the West African subregion.

Key words: climate adaptation, climate change, CORDEX, Ghana, RCPs, Savannah zone

HIGHLIGHTS

- The performance of six RCMs participating in the CORDEX-Africa initiative was assessed.
- Accuracy of both RCMs and their ensemble mean improved with bias correction.
- The overall changes in projected annual precipitation reveal a general decline in rainfall.
- The mean temperature changes recorded show a general increase.
- This study serves as a guide for Ghana and West Africa in planning cost-effective climate adaptation strategies.

GRAPHICAL ABSTRACT



1. INTRODUCTION

Over the past century, climate studies have intensified as scientists work tirelessly to understand climate changes and their impacts on future climate (IPCC 2007; Giménez & García-Galiano 2018). The African continent, in particular, is identified as the most vulnerable to climate change and its impacts due to the high dependence of livelihoods and various sectors of the economies on climate (IPCC 2007; Kalognomou *et al.* 2013; Yira *et al.* 2017). Consequently, irregularities in the climate negatively affect livelihoods (Boko *et al.* 2008; Kalognomou *et al.* 2013; Thornton *et al.* 2014), and there is a need for proper planning and implementation of sound policies to enhance sustainable adaptation and coping mechanisms. Understanding the impacts of future climate becomes an asset in managing these vulnerabilities.

In Africa, the vulnerability to climate change has been well documented, with many livelihoods and economic sectors heavily dependent on the climate. Recent studies have highlighted the impact of climate change on African agriculture and food security (Schlenker & Lobell 2010; Lobell *et al.* 2013), as well as the increased risk of conflict and displacement due to climate-related disasters (Käkönen 2020). This vulnerability of the African continent to climate change poses a threat to achieving sustainable development goals. Many of the goals, such as eradicating poverty (Goal 1), achieving food security (Goal 2), ensuring good health and well-being (Goal 3), and promoting sustainable economic growth (Goal 8), are dependent on climate stability. The impacts of climate change, such as extreme weather events, sea-level rise, and changes in precipitation patterns, can lead to food shortages, displacement of populations, and increased poverty.

The projection of future climate often involves the use of climate models, which are mathematical equations that run on a three-dimensional grid (Intergovernmental Panel on Climate Change (IPCC) 2001; Rajib & Rahman 2012). General circulation models (GCMs) are one group of climate models that are often used in climate change studies, but they have a resolution of 200 km or more, which limits their ability to estimate changes in future climate at the regional scale. Either they are unable to capture mesoscale atmospheric circulations or the intensities they present are unrealistic (Christensen *et al.* 2007; Kendon *et al.* 2010; Rajib & Rahman 2012). Atmosphere-ocean GCMs (AOGCMs) are reported to produce relatively good predictions, especially on flat, noncoastal terrains (Kendon *et al.* 2010). However, these AOGCMs inadequately simulate the underlying West African monsoon (WAM) rainfall, which is the basis of the general rainfall pattern in West Africa (Hourdin *et al.* 2010; Xue *et al.* 2010; Gbobaniyi *et al.* 2014).

Regional climate models (RCMs), with a finer resolution (50 km), have been applied for West Africa and have relatively simulated the WAM climatology quite well (Afiesimama *et al.* 2006; Foamouhou & Buscarlet 2006; Pal *et al.* 2007; Sylla *et al.* 2009). However, the use of single RCMs often results in some biases (Christensen *et al.* 2008; Teutschbein & Seibert 2012) due to the model used, the region of analysis, or the season under consideration (Nikulin *et al.* 2012). The use of multi-model average (ensemble mean) together with bias-correction methods has been found to enhance the performance of simulations (Teutschbein & Seibert 2010; Diallo *et al.* 2011; Paeth *et al.* 2011; Nikulin *et al.* 2012; Johnson & Sharma 2015).

In terms of climate modeling, recent studies have continued to focus on improving the accuracy of RCMs. For example, a study by Akinsanola *et al.* (2021) evaluated the performance of several RCMs in simulating the WAM and found that a multi-model ensemble approach provided the most accurate simulations. Another study by Safari *et al.* (2021) evaluated the performance of RCMs in simulating rainfall over Rwanda and found that a bias-correction approach improved the accuracy of the simulations.

In this study, the performance of six individual RCMs participating in the Coordinated Regional Climate Downscaling Experiment (CORDEX)-Africa project and their multimodel average (ensemble mean) were evaluated, as well as their performance before and after bias correction was applied to their outputs. The analysis included the comparison of monthly means with observations for both temperature and rainfall. Furthermore, these RCMs were used to project the future climate (temperature and rainfall) for the SADA zone of Ghana.

2. MATERIALS AND METHODS

2.1. Study area

The area demarked as the Savannah zone covers the Upper West, Upper East, North East, Northern, Savannah, parts of Bono East, and Oti regions of Ghana (Figure 1). The area lies within latitudes 8°00'N– 11°00'N and longitudes 0°01'E–3°

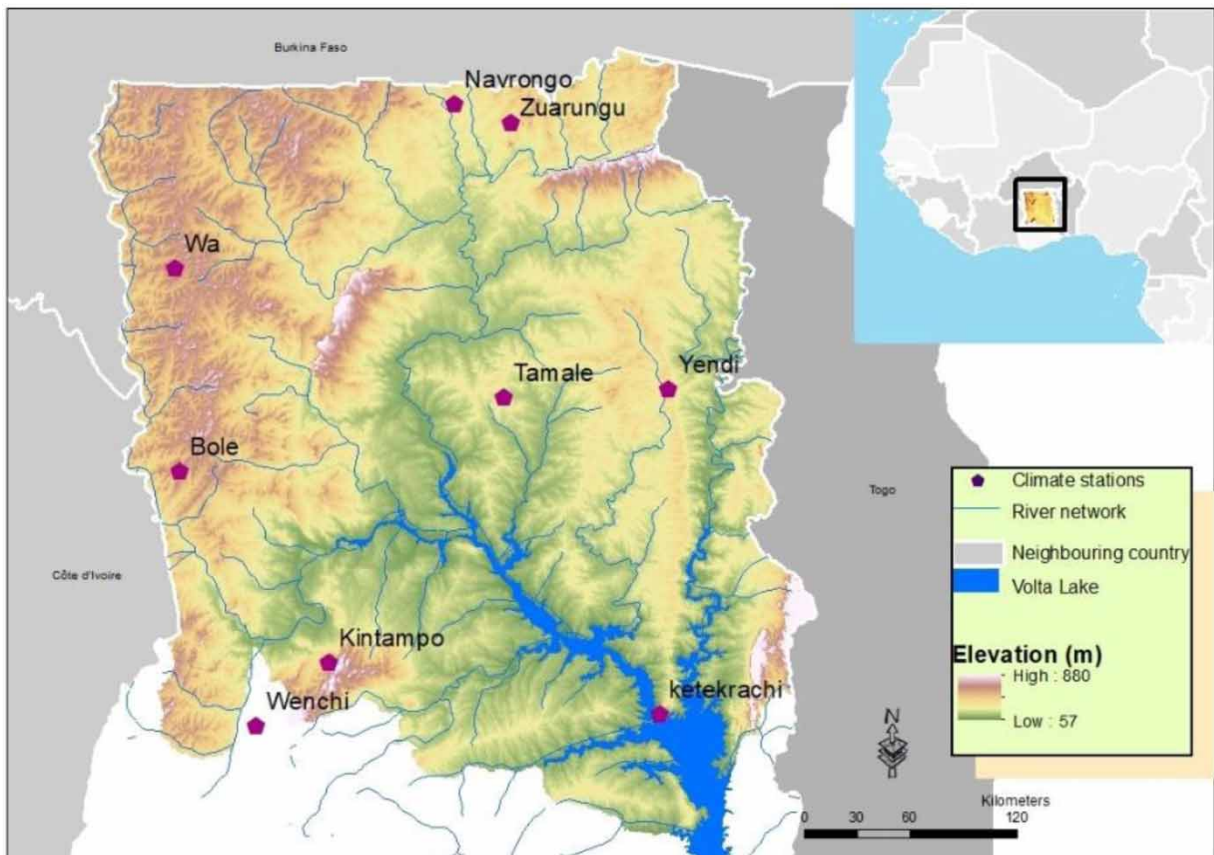


Figure 1 | Location of climate stations in the Savannah zone of Ghana.

00°W. The climate in the study area is primarily semiarid in the northern parts, semihumid in the central regions, and then humid in the southern parts (Liebe *et al.* 2009). Rainfall is characterized by significant variations, including disparities between successive seasons, and is often unpredictable in terms of onset, quantity, and coverage (Obuobie 2008; Ghansah *et al.* 2018). In the northern part, the mean monthly temperature falls between 27 and 36 °C, and in the southern part, it ranges from 24 to 34 °C, while relatively high evapotranspiration rates are observed with potential evapotranspiration rates exceeding mean annual rainfall amounts (Darko *et al.* 2018).

The primary vegetation of the SADA zone is mainly Savannah consisting of grasslands dotted with trees/shrubs such as the baobab, shea, mango, and neem. The southern parts are, however, characterized by dry forests that have a few tall trees with shrubs and grasses growing underneath (Darko 2018).

A large percentage of the inhabitants in the SADA zone are peasant farmers living in scattered rural communities (Darko 2018). The farmers are highly defenseless against upsets due to the limited augmentation of their income sources (World Bank 2011). Thus, any slight variation in the climate often results in poverty, hunger, and high competition for the limited available resources (Mul *et al.* 2015). Table 1 shows the description of the selected stations for the study.

2.2. Baseline data

Daily precipitation values for the baseline period of 1960–2005 for precipitation and 1975–2005 for temperature runs were obtained from the Ghana Meteorological Agency. These periods were selected because of the availability of observed data and also because the baseline period for the CORDEX-Africa projects ends in 2005.

2.3. Climate change data

RCM simulations utilized were daily precipitation and temperature values obtained from RCMs participating in the CORDEX-Africa projects (Jones *et al.* 2011). An ensemble of six RCM–GCM (Table 2) as well as their multimodel average (ensemble mean) were used in the analysis.

The ability of the models to accurately model future climate was tested by assessing their performance in simulating observed data. This test was necessary because models cannot be relied on to project future climate if they are unable to accurately simulate observed climate (Laprise *et al.* 2013). The representative concentration pathway (RCP) scenarios 4.5 and 8.5 of the Intergovernmental Panel on Climate Change were utilized in the projection of future climate.

Bias correction was employed using the climate model data for hydrologic modeling tool. Further details about the tool can be found in Rathjens *et al.* (2016). Bias correction was carried out because climate models tend to produce a biased representation of the observation (Christensen *et al.* 2008; Teutschbein & Seibert 2012). This is because simulations by RCMs are limited in their ability to accurately capture all the physical and chemical processes that occur in the atmosphere (Lupo & Kininmonth 2013).

The distribution mapping, which is a type of gamma method of bias correction, was chosen for both precipitation and temperature. This method works by correcting the distribution function of the simulations from the RCM to align with that of the observations (Sennikovs & Bethers 2009; Teutschbein & Seibert 2012). This method of bias correction has also proven to

Table 1 | Description of climate stations used in the study

| Climate station | Longitude | Latitude | Elevation |
|-----------------|-----------|----------|-----------|
| Bole | −2.49 | 9.03 | 297.00 |
| Kete-Krachi | −0.05 | 7.80 | 85.00 |
| Kintampo | −1.73 | 8.06 | 339.00 |
| Tamale | −0.84 | 9.24 | 196.00 |
| Wa | −2.51 | 10.06 | 305.00 |
| Wenchi | −2.10 | 7.74 | 304.00 |
| Zuarungu | −0.81 | 10.80 | 213.00 |
| Navrongo | −1.09 | 10.89 | 196.00 |
| Yendi | −0.01 | 9.45 | 252.00 |

Note: Latitude and longitudes in decimal degrees, elevation in meters.

Table 2 | Details of RCMS used in this study

| Model | Driving GCM | RCM institute | Adopted Id |
|-------|------------------|--|---------------|
| REMO | MPI-M-MPI-ESM-LR | Climate Service Centre in Hamburg, Germany (CSC) | REMO-MPI |
| RCA4 | MOHC-HadGEM2-ES | Swedish Meteorological and Hydrological Institute (SMHI) | RCA4-HadGEM2 |
| RCA4 | CCCma-CanESM2 | Swedish Meteorological and Hydrological Institute (SMHI) | RCA4-CanESM2 |
| HIRAM | NCC-NorESM1-M | Danish Meteorological Institute (DMI) | HIRAM-NorESM1 |
| RACMO | ICHEC-EC-EARTH | Royal Netherlands Meteorological Institute (KNMI) | RACMO-EARTH |
| RCA4 | NOAA | North American Space Agency | RCA4-NOAA |

have high-performance ability in correcting most of the statistical characteristics of the RCM (Teutschbein & Seibert 2012, 2013; Ibebuchie 2021, 2022).

2.4. Statistical analysis

Statistical parameters, namely, root mean square error (RMSE), mean absolute error (MAE), and coefficient of determination (R^2), were used to assess the performance of RCMS. The RMSE and MAE measure the error between the observed data and the simulated data. It is thus postulated that the smaller value (i.e., the closer it is to zero), the better or closer the stimulation value to the observed data. These parameters have been widely accepted and employed in measuring model performance in climate studies (Bennett *et al.* 2013; Amirabadizadeh *et al.* 2016).

RCM outputs without bias correction and those that underwent bias correction are hereafter referred to as raw and bias corrected, respectively.

Each RCM was evaluated to determine how well they were able to simulate the past climate. The ensemble means of these RCMS were also tested to see their ability in reproducing past climatic features.

3. RESULTS

3.1. Model performance (rainfall)

RCMS simulated observed rainfall with varying levels of accuracy, as was also observed by Nikulin *et al.* (2012). Uncertainties in the reproduction of the observed rainfall by the raw RCMS varied across stations (Table 3). RC4A-HadGEM2 had the highest RMSE and MAE values of 86–124 and 11–70 mm, respectively, for the highest number of stations (six stations), indicative of the highest error margins and thus be said to be the least performing model. RCA4-NOAA also recorded relatively high RMSE and MAE values for the second highest number (four stations) of stations, and REMO-MPI also recorded relatively high RMSE and MAE values for three stations.

The R^2 of the raw RCMS ranged from 0.69 to 0.99 (Table 3). Most of the raw RCMS' R^2 values were higher than 0.50 for all the stations except Tamale, where all the raw RCMS recorded relatively low values ranging from 0.07 to 0.89 with REMO-MPI recording the lowest value of 0.07. The R^2 ranges typically from 0 to 1 and is a measure of how well the models can simulate the observed data. Values of R^2 closer to 1 are considered the best simulations, but values >0.50 are generally regarded as acceptable (Santhi *et al.* 2001; Van Liew *et al.* 2003). However, per the observed simulation and comparison with the other performance estimators, using the R^2 alone as a performance indicator may be misleading.

The ensemble means of the raw RCMS captured the rainfall patterns (peaks) better than most of the individual RCMS, although with varying levels of uncertainties across the stations. The RMSE and MAE for the ensemble means showed that even for the raw outputs, it performed relatively better than most individual RCMS. The values recorded ranged from 19 to 76 mm and 13 to 63 mm, respectively, for RMSE and MAE, for all RCMS at all locations (Table 3). Tamale recorded the highest value of 76 and 63 mm for both RMSE and MAE, respectively. The R^2 analysis showed values that ranged from 0.69 to 0.99.

The accuracy of individual RCMS improved with bias correction. RMSE and MAE values ranged from 2 to 23 mm and 2 to 22 mm, respectively. Most of the stations recorded values less than 10 mm for all bias-corrected RCMS, apart from Kete-Krachi, where all the RCMS recorded relatively high values for both RMSE and MAE, with RACMO-EARTH recording the highest value of 22 mm for RMSE. In contrast, RCA4-CanESM1 and RCA4-NOAA recorded 23 mm for MAE (Table 3).

Table 3 | R^2 , RMSE (mm), MAE (mm), and standard deviation of the raw and bias-corrected (in parenthesis) simulations of rainfall, maximum and minimum temperature of the individual RCMs, and their ensemble mean for each location

| | R^2 | | | RMSE (mm) | | | MAE (mm) | | | Standard deviation | | |
|--------------------|--------|-----------|-----------|-----------|-----------|-----------|----------|-----------|-----------|--------------------|-----------|-----------|
| | Prcp | T_{max} | T_{min} | Prcp | T_{max} | T_{min} | Prcp | T_{max} | T_{min} | Prcp | T_{max} | T_{min} |
| Bole | | | | | | | | | | | | |
| RCA4-CanESM2 | 0.62 | 0.78 | 0.74 | 48 | 4 | 2 | 35 | 4 | 2 | 44.4 | 1.3 | 1.8 |
| | [1.00] | [1.0] | [1.0] | [9] | [0] | [0] | [7] | [0] | [0] | [6.7] | [0.0] | [0.0] |
| RCA4-HadGEM2 | 0.86 | 0.77 | 0.54 | 95 | 4 | 3 | 86 | 4 | 3 | 99.0 | 4.4 | 3.2 |
| | [1.00] | [1.0] | [1.0] | [4] | [0] | [0.0] | [3] | [0] | [0.0] | [2.3] | [0.0] | [0.0] |
| RACMO-EARTH | 0.91 | 0.90 | 0.71 | 27 | 4 | 3 | 21 | 3 | 3 | 25.4 | 0.9 | 1.3 |
| | [0.97] | [1.0] | [1.0] | [13] | [0] | [0] | [9] | [0] | [0] | [13.4] | [0.0] | [0.0] |
| REMO-MPI | 0.84 | 0.41 | 0.61 | 85 | 2 | 2 | 62 | 2 | 2 | 79.3 | 2.4 | 2.1 |
| | [1.00] | [1.0] | [1.0] | [12] | [0] | [0] | [9] | [0] | [0] | [8.6] | [0.0] | [0.0] |
| RCA4-NOAA | 0.87 | 0.90 | 0.68 | 34 | 2 | 3 | 28 | 2 | 2 | 34.2 | 0.9 | 1.7 |
| | [0.99] | [1.0] | [1.0] | [14] | [0] | [0] | [10] | [0] | [0] | [12.0] | [0.0] | [0.0] |
| HIRAM-NorESM1 | 0.96 | 0.88 | 0.75 | 47 | 2 | 4 | 37 | 1 | 4 | 38.1 | 3.5 | 1.0 |
| | [1.00] | [1.0] | [1.0] | [8] | [0] | [0] | [7] | [0] | [0] | [6.3] | [0.0] | [0.0] |
| Ensemble Mean | 0.94 | 0.74 | 0.86 | 19 | 2 | 1 | 14 | 1 | 1 | 16.7 | 1.6 | 1.0 |
| | [1.00] | [1] | [1.0] | [8] | [0] | [0] | [6] | [0] | [0] | [6.1] | [0.0] | [0.0] |
| Kete-Krachi | | | | | | | | | | | | |
| RCA4-CanESM2 | 0.50 | 0.92 | 0.92 | 84 | 3 | 3 | 59.2 | 3 | 3 | 68 | 0.8 | 2.5 |
| | [0.94] | [1.0] | [1.0] | [23] | [0] | [0] | [18] | [0] | [0] | [24] | [0.0] | [0.0] |
| RCA4-HadGEM2 | 0.85 | 0.73 | 0.73 | 117 | 4 | 4 | 104.8 | 4 | 4 | 117 | 4.0 | 2.7 |
| | [0.96] | [1.0] | [1.0] | [19] | [0] | [0] | [14] | [0] | [0] | [19.6] | [0.0] | [0.0] |
| RACMO-EARTH | 0.68 | 0.66 | 0.66 | 54 | 3 | 3 | 43.3 | 2 | 2 | 54 | 1.7 | 0.8 |
| | [0.94] | [1.0] | [1.0] | [17] | [0] | [0] | [22] | [0] | [0] | [23.2] | [0.0] | [0.0] |
| REMO-MPI | 0.90 | 0.93 | 0.93 | 80 | 1 | 1 | 50.4 | 1 | 1 | 75 | 0.6 | 1.0 |
| | [0.96] | [1.0] | [1.0] | [20] | [0] | [0] | [16] | [0] | [0] | [20.0] | [0.0] | [0.0] |
| RCA4-NOAA | 0.80 | 0.97 | 0.97 | 52 | 2 | 2 | 39.4 | 1 | 1 | 44 | 0.9 | 2.4 |
| | [0.96] | [1.0] | [1.0] | [23] | [0] | [0] | [20] | [0] | [0] | [22.6] | [0.0] | [0.0] |
| HIRAM-NorESM1 | 0.95 | 0.96 | 0.96 | 38 | 2 | 2 | 26.4 | 2 | 2 | 31 | 0.7 | 1.3 |
| | [0.96] | [1.0] | [1.0] | [18] | [0] | [0] | [13] | [0] | [0] | [19.0] | [0.0] | [0.0] |
| Ensemble mean | 0.96 | 0.96 | 0.96 | 32 | 1 | 1 | 25.8 | 1 | 1 | 31 | 0.5 | 0.7 |
| | [0.96] | [1.0] | [1.0] | [19] | [0] | [0] | [14] | [0.0] | [0] | [20.0] | [0.0] | [0.0] |
| Kintampo | | | | | | | | | | | | |
| RCA4-CanESM2 | 0.49 | | | 66 | | | 66 | | | 86.4 | | |
| | [1.0] | | | [5] | | | [4] | | | [4.7] | | |
| RCA4-HadGEM2 | 0.67 | | | 98 | | | 98 | | | 117.1 | | |
| | [1.0] | | | [2] | | | [2] | | | [2.5] | | |
| RACMO-EARTH | 0.75 | | | 28 | | | 28 | | | 39.4 | | |
| | [0.99] | | | [8] | | | [6] | | | [7.8] | | |
| REMO-MPI | 0.51 | | | 73 | | | 73 | | | 65.5 | | |
| | [1.0] | | | [3] | | | [2] | | | [2.6] | | |

(Continued.)

Table 3 | Continued

| | R^2 | | | RMSE (mm) | | | MAE (mm) | | | Standard deviation | | |
|-----------------|--------|-----------|-----------|-----------|-----------|-----------|----------|-----------|-----------|--------------------|-----------|-----------|
| | Prcp | T_{max} | T_{min} | Prcp | T_{max} | T_{min} | Prcp | T_{max} | T_{min} | Prcp | T_{max} | T_{min} |
| RCA4-NOAA | 0.74 | | | 70 | | | 70 | | | 82.6 | | |
| | [1.0] | | | [9] | | | [7] | | | [8.5] | | |
| HIRAM-NorESM1 | 0.86 | | | 47 | | | 38 | | | 40.2 | | |
| | [1.0] | | | [4] | | | [3] | | | [3.0] | | |
| Ensemble mean | 0.78 | | | 31 | | | 31 | | | 36.7 | | |
| | [1.0] | | | [2] | | | [2] | | | [2.1] | | |
| Navrongo | | | | | | | | | | | | |
| RCA4-CanESM2 | 0.67 | 0.79 | 0.70 | 51 | 2 | 2 | 36 | 1 | 2 | 52.9 | 1.4 | 2.0 |
| | [1.0] | [1.0] | [1.0] | [6] | [0.0] | [0] | [4] | [0.0] | [0] | [4.8] | [0.0] | [0.0] |
| RCA4-HadGEM2 | 0.78 | 0.52 | 0.61 | 124 | 5 | 4 | 111 | 4 | 3 | 126.4 | 4.6 | 3.8 |
| | [1.0] | [1.0] | [1.0] | [3] | [0.0] | [0] | [2] | [0.0] | [0] | [3.4] | [0.0] | [0.0] |
| RACMO-EARTH | 0.75 | 0.57 | 0.71 | 49 | 5 | 3 | 33 | 5 | 3 | 81.3 | 2 | 1.3 |
| | [0.99] | [1.0] | [1.0] | [10] | [0.0] | [0] | [7] | [0.0] | [0] | [10.5] | [0.0] | [0.0] |
| REMO-MPI | 0.81 | 0.77 | 0.62 | 59 | 2 | 2 | 32 | 1 | 2 | 117.2 | 1.4 | 1.9 |
| | [1.0] | [1.0] | [1.0] | [5] | [0.0] | [0] | [4] | [0.0] | [0] | [4.2] | [0.0] | [0.0] |
| RCA4-NOAA | 0.79 | 0.83 | 0.69 | 51 | 2 | 3 | 37 | 1 | 2 | 96.3 | 1.3 | 1.9 |
| | [1.0] | [1.0] | [1.0] | [9] | [0.0] | [0] | [6] | [0.0] | [0] | [7.5] | [0.0] | [0.0] |
| HIRAM-NorESM1 | 0.83 | 0.91 | 0.65 | 74 | 1 | 5 | 54 | 1 | 4 | 123.0 | 1 | 1.3 |
| | [1.0] | [1.0] | [1.0] | [5] | [0.0] | [0] | [3] | [0.0] | [0] | [4.8] | [0.0] | [0.0] |
| Ensemble mean | 0.87 | 0.88 | 0.76 | 43 | 2 | 1 | 38 | 1 | 1 | 45.5 | 36.3 | 1.1 |
| | [1.0] | [1.0] | [1.0] | [4] | [0.0] | [0] | [2] | [0.0] | [0] | [3.7] | [0.0] | [0.0] |
| Tamale | | | | | | | | | | | | |
| RCA4-CanESM2 | 0.89 | 0.73 | 0.09 | 108 | 18 | 15 | 90 | 15 | 15 | 101.1 | 7.9 | 5.4 |
| | [1.0] | [1.0] | [1.0] | [5] | [0] | [0] | [3] | [0] | [0] | [5.3] | [2.9] | [0.0] |
| RCA4-HadGEM2 | 0.54 | 0.31 | 0.41 | 86 | 16 | 15 | 70 | 15 | 14 | 76.8 | 6.0 | 5.9 |
| | [1.0] | [1.0] | [1.0] | [2] | [0.0] | [0] | [2] | [0.0] | [0] | [2.2] | [2.9] | [0.0] |
| RACMO-EARTH | 0.13 | 0.78 | 0.07 | 91 | 20 | 17 | 73 | 18 | 17 | 87.4 | 6.4 | 4.7 |
| | [1.0] | [1.0] | [1.0] | [5] | [0] | [0] | [4] | [0] | [0] | [5.4] | [2.9] | [0.0] |
| REMO-MPI | 0.07 | 0.78 | 0.07 | 87 | 19 | 15 | 71 | 17 | 14 | 85.9 | 6.4 | 4.5 |
| | [0.99] | [1.0] | [1.0] | [10] | [0] | [0] | [5] | [0] | [0] | [10.1] | [2.9] | [0.0] |
| RCA4-NOAA | 0.28 | 0.73 | 0.09 | 87 | 20 | 16 | 73 | 18 | 16 | 88.0 | 6.2 | 4.3 |
| | [1.0] | [1.0] | [1.0] | [4] | [0] | [0] | [3] | [0] | [0] | [3.5] | [2.9] | [0.0] |
| HIRAM-NorESM1 | | 0.66 | 0.12 | | 18 | 12 | | 15 | 11 | | 6.9 | 4.8 |
| | | [1.0] | [1.0] | | [0] | [0.0] | | [0] | [0] | | [2.9] | [0.0] |
| Ensemble mean | 0.69 | 0.81 | 0.04 | 76 | 18 | 15 | 63 | 16 | 15 | 73.0 | 4.8 | 3.7 |
| | [1.0] | [1.0] | 1.00 | [5] | [0] | 0.0 | [3] | [0] | 0.0 | [4.9] | [2.9] | 0.0 |
| Wa | | | | | | | | | | | | |
| RCA4-CanESM2 | 0.69 | 0.83 | 0.4 | 46 | 2 | 2.9 | 32 | 2 | 2.5 | 43.7 | 1.1 | 2.8 |
| | [1.0] | [1.0] | [1.0] | [4] | [0] | [0] | [3] | [0] | [0] | [3.7] | [0.0] | [0.0] |
| RCA4-HadGEM2 | 0.85 | 0.69 | 0.4 | 105 | 4 | 3.5 | 95 | 4 | 2.9 | 109.8 | 4.2 | 3.3 |
| | [1.0] | [1.0] | [1.0] | [3] | [0] | [0] | [2] | [0] | [0] | [3.1] | [0.0] | [0.0] |

(Continued.)

Table 3 | Continued

| | R^2 | | | RMSE (mm) | | | MAE (mm) | | | Standard deviation | | |
|---------------|--------|-----------|-----------|-----------|-----------|-----------|----------|-----------|-----------|--------------------|-----------|-----------|
| | Prcp | T_{max} | T_{min} | Prcp | T_{max} | T_{min} | Prcp | T_{max} | T_{min} | Prcp | T_{max} | T_{min} |
| RACMO-EARTH | 0.94 | 0.86 | 0.6 | 29 | 4 | 3.5 | 22 | 4 | 3.1 | 23.6 | 1.0 | 1.7 |
| | [0.99] | [1.0] | [1.0] | [9] | [0] | [0] | [7] | [0] | [0] | [8.8] | [0] | [0.0] |
| REMO-MPI | 0.91 | 0.34 | 0.5 | 59 | 3 | 2.7 | 42 | 2 | 2.4 | 55.9 | 2.6 | 2.7 |
| | [1.0] | [1.0] | [1.0] | [5] | [0] | [0] | [5] | [0] | [0] | [5.1] | [0.0] | [0.0] |
| RCA4-NOAA | 0.93 | 0.94 | 0.5 | 29 | 1 | 3.6 | 22 | 1 | 2.7 | 27.0 | 0.7 | 2.5 |
| | [1.0] | [1.0] | [1.0] | [7] | [0.0] | [0] | [5] | [0] | [0] | [6.9] | [0.0] | [0.0] |
| HIRAM-NorESM1 | 0.97 | 0.83 | 1.0 | 43 | 2 | 4.3 | 31 | 2 | 4.3 | 34.7 | 1.1 | 0.4 |
| | [1.0] | [1.0] | [1.0] | [5] | [0] | [0] | [3] | [0] | [0] | [4.7] | [0.0] | [0.0] |
| Ensemble mean | 0.99 | 0.80 | 0.6 | 14 | 1 | 1.5 | 13 | 1 | 1.3 | 9.8 | 1.3 | 1.4 |
| | [1.0] | [1.0] | [1.0] | [3] | [0] | [0] | [3] | [0] | [0] | [3.3] | [0.0] | [0.0] |
| Wenchi | | | | | | | | | | | | |
| RCA4-CanESM2 | 0.53 | 0.84 | 0.4 | 58 | 4 | 3.1 | 41 | 3 | 2.9 | 48.0 | 1.1 | 3.2 |
| | [0.99] | [1.0] | [1.0] | [7] | [0] | [0] | [6] | [0] | [0] | [6.2] | [3.4] | [0.0] |
| RCA4-HadGEM2 | 0.61 | 0.58 | 0.2 | 88 | 4 | 2.2 | 80 | 3 | 1.9 | 89.1 | 3.8 | 2.3 |
| | [0.99] | [1.0] | [1.0] | [5] | [0] | [0] | [4] | [0] | [0] | [5.3] | [12.8] | [0.0] |
| RACMO-EARTH | 0.78 | 0.74 | 0.5 | 35 | 2 | 2.0 | 26 | 2 | 1.4 | 31.8 | 1.3 | 1.5 |
| | [0.98] | [1.0] | [1.0] | [10] | [0] | [0] | [8] | [0] | [0] | [107] | [4.1] | [0.0] |
| REMO-MPI | 0.56 | 0.76 | 0.4 | 94 | 2 | 2.3 | 73 | 2 | 2.1 | 92.2 | 1.5 | 2.2 |
| | [0.99] | [1.0] | [1.0] | [6] | [0] | [0] | [6] | [0] | [0] | [6.3] | [4.6] | [0.0] |
| RCA4-NOAA | 0.64 | 0.94 | 0.4 | 48 | 2 | 3.3 | 35 | 2 | 2.4 | 49.5 | 1.1 | 3.1 |
| | [0.99] | [1.0] | [1.0] | [10] | [0] | [0] | [9] | [0] | [0] | [9.6] | [3.3] | [0.0] |
| HIRAM-NorESM1 | 0.64 | 0.98 | 0.8 | 46 | 2 | 5.1 | 39 | 2 | 5.0 | 48.2 | 0.6 | 0.7 |
| | [1.0] | [1.0] | [1.0] | [4] | [0] | [0] | [3] | [0] | [0] | [4.0] | [1.7] | [0.0] |
| Ensemble mean | 0.71 | 0.98 | 0.5 | 36 | 2 | 1.4 | 29 | 2 | 1.4 | 36.5 | 0.4 | 1.4 |
| | [1.0] | [1.0] | [1.0] | [4] | [0] | [0] | [3] | [0] | [0] | [3.6] | [1.5] | [0.0] |
| Yendi | | | | | | | | | | | | |
| RCA4-CanESM2 | 0.60 | 0.86 | 0.57 | 62 | 2 | 2 | 42 | 2 | 2 | 60.2 | 1.1 | 2.4 |
| | [1.0] | [1.0] | [1.0] | [7] | [0] | [0] | [5] | [0] | [0] | [6.6] | [0] | [0.0] |
| RCA4-HadGEM2 | 0.81 | 0.71 | 0.49 | 124 | 4 | 3 | 111 | 4 | 3 | 129.7 | 4.6 | 3.3 |
| | [1.0] | [1.0] | [1.0] | [4] | [0] | [0] | [3] | [0] | [0] | [3.8] | [0] | [0.0] |
| RACMO-EARTH | 0.80 | 0.81 | 0.65 | 41 | 4 | 3 | 27 | 4 | 2 | 42.6 | 1.2 | 1.5 |
| | [0.98] | [1.0] | [1.0] | [11] | [0] | [0] | [8] | [0] | [0] | [11.7] | [0] | [0.0] |
| REMO-MPI | 0.93 | 0.64 | 0.51 | 35 | 2 | 2 | 26 | 2 | 2 | 35.5 | 1.8 | 2.2 |
| | [1.0] | [1.0] | [1.0] | [11] | [0] | [0] | [9] | [0] | [0] | [9.2] | [0] | [0.0] |
| RCA4-NOAA | 0.86 | 0.95 | 0.56 | 35 | 1 | 3 | 23 | 1 | 2 | 36.0 | 0.7 | 2.3 |
| | [1.0] | [1.0] | [1.0] | [6] | [0] | [0] | [4] | [0] | [0] | [6.0] | [0] | [0.0] |
| HIRAM-NorESM1 | 0.95 | 0.96 | 0.77 | 47 | 1 | 5 | 35 | 1 | 5 | 38.0 | 0.6 | 0.8 |
| | [1.0] | [1.0] | [1.0] | [6] | [0] | [0] | [5] | [0] | [0] | [6.1] | [0] | [0.0] |
| Ensemble mean | 0.94 | 0.92 | 0.96 | 29 | 1 | 1 | 24 | 1 | 1 | 29.7 | 1.0 | 1.1 |
| | [1.0] | [1.0] | [1.0] | [4] | [0] | [0] | [3] | [0] | [0] | [3.9] | [0] | [0.0] |

(Continued.)

Table 3 | Continued

| | R^2 | | | RMSE (mm) | | | MAE (mm) | | | Standard deviation | | |
|-----------------|-------|-----------|-----------|-----------|-----------|-----------|----------|-----------|-----------|--------------------|-----------|-----------|
| | Prcp | T_{max} | T_{min} | Prcp | T_{max} | T_{min} | Prcp | T_{max} | T_{min} | Prcp | T_{max} | T_{min} |
| Zuarungu | | | | | | | | | | | | |
| RCA4-CanESM2 | 0.60 | 0.56 | 0.59 | 60 | 2 | 2 | 42 | 2 | 2 | 56.6 | 2.1 | 1.9 |
| | [1.0] | [1.0] | [1.0] | [4] | [0] | [0] | [3] | [0] | [0] | [3.6] | [0.0] | [0.0] |
| RCA4-HadGEM2 | 0.83 | 0.62 | 0.55 | 115 | 4 | 3 | 103 | 4 | 2 | 119.9 | 4.4 | 2.9 |
| | [1.0] | [1.0] | [1.0] | [5] | [0] | [0] | [3] | [0] | [0] | [5.0] | [0] | [0.1] |
| RACMO-EARTH | 0.92 | 0.78 | 0.64 | 37 | 5 | 4 | 27 | 5 | 3 | 29.7 | 1.5 | 1.8 |
| | [1.0] | [1.0] | [1.0] | [5] | [0] | [0] | [3] | [0] | [0] | [3.8] | [0.0] | [0.0] |
| REMO-MPI | 0.95 | 0.26 | 0.47 | 34 | 3 | 3 | 22 | 3 | 3 | 33.2 | 3.2 | 3.2 |
| | [1.0] | [1.0] | [1.0] | [4] | [0.0] | [0] | [4] | [0] | [0] | [4.0] | [0.0] | [0.0] |
| RCA4-NOAA | 0.83 | 0.79 | 0.66 | 36 | 1 | 2 | 24 | 1 | 2 | 37.4 | 1.4 | 1.6 |
| | [1.0] | [1.0] | [1.0] | [6.] | [0] | [0] | [5] | [0] | [0] | [5] | [0.0] | [0.0] |
| HIRAM-NorESM1 | 0.98 | 0.68 | 0.90 | 31 | 2 | 5 | 23 | 2 | 4 | 23.5 | 1.8 | 1.0 |
| | [1.0] | [1.0] | [1.0] | [6] | [0] | [0] | [4] | [0] | [0] | [5.8] | [0.0] | [0.0] |
| Ensemble mean | 0.96 | 0.64 | 0.67 | 21 | 2 | 1 | 25 | 2 | 1 | 25.4 | 2.0 | 1.3 |
| | [1.0] | [1.0] | [1.0] | [3] | [0] | [0] | [2] | [0] | [0] | [2.6] | [0.0] | [0.0] |

R^2 values of the bias-corrected RCMs ranged from 0.94 to 1.00 for all RCMs at all stations (Table 3). Kete-Krachi recorded the lowest R^2 values (0.94) recorded by RCA4-CanESM2 and RACMO-EARTH (Table 3). As mentioned earlier, the closer the R^2 value is to 1 indicates a lower level of error by the model in simulating the observed data. Thus, the performance of the models in simulating the observed data is seen to improve with bias correction as was critically pointed out by Teutschbein & Seibert (2012).

Similar to the observation made for the individual RCMs, the performance of the ensemble means improved with bias correction. RMSE values ranged from 2 to 19 mm for all stations (Table 3). The highest value of 19 mm was recorded at Kete-Krachi with the rest of the stations having values less than 10 mm. MAE values obtained after bias correction also ranged from 2 to 14 mm with Kete-Krachi again recording the highest value of 14 mm. The remainder of the stations had values less or equal to 6 mm. These indicate that the removal of biases from the simulated data improved the similarity between these and the observed data.

3.2. Simulation of monthly rainfall

The monthly simulations of rainfall patterns for each climate station per each RCM are presented in Figure 2. RCMs were mostly unable to simulate the rainfall patterns correctly. For stations with two peaks in their cycle (Bole, Kete-Karachi, and Wenchi), most of the individual RCMs either failed to detect the two peaks or simulated a third peak. For such stations, RCA-4 CanESM2 did a better job at mimicking the peaks better than the other RCMs, although with high underestimations of the rainfall amounts. For the other stations (Navrongo, Tamale, Wa, Yendi, and Zuarungu) with just one peak, REMO-MPI did better at simulating this pattern as compared to the other RCMs, albeit with some level of overestimation. RCA4-HadGEM2 was the only RCM that was unable to capture the monthly rainfall pattern present in the observed data for all the stations.

However, for stations such as Tamale and Kintampo, neither the raw RCMs nor their ensemble mean was able to capture the rainfall pattern in the observed data (Figure 2). For Tamale, all the RCMs overpredicted the rainfall from October to March and then underpredicted it from April to September. At Kintampo on the other hand, all the raw RCMs excluding RCA4-NOAA, HIRAM-NORESM1, and RCA4-CanESM2 underpredicted the observed data for all the months (Figure 2).

The lowest underestimations in simulated data were recorded from November to March. These months fall within the dry season of the study area. On the other hand, overestimations generally occurred from April to October, when most of the

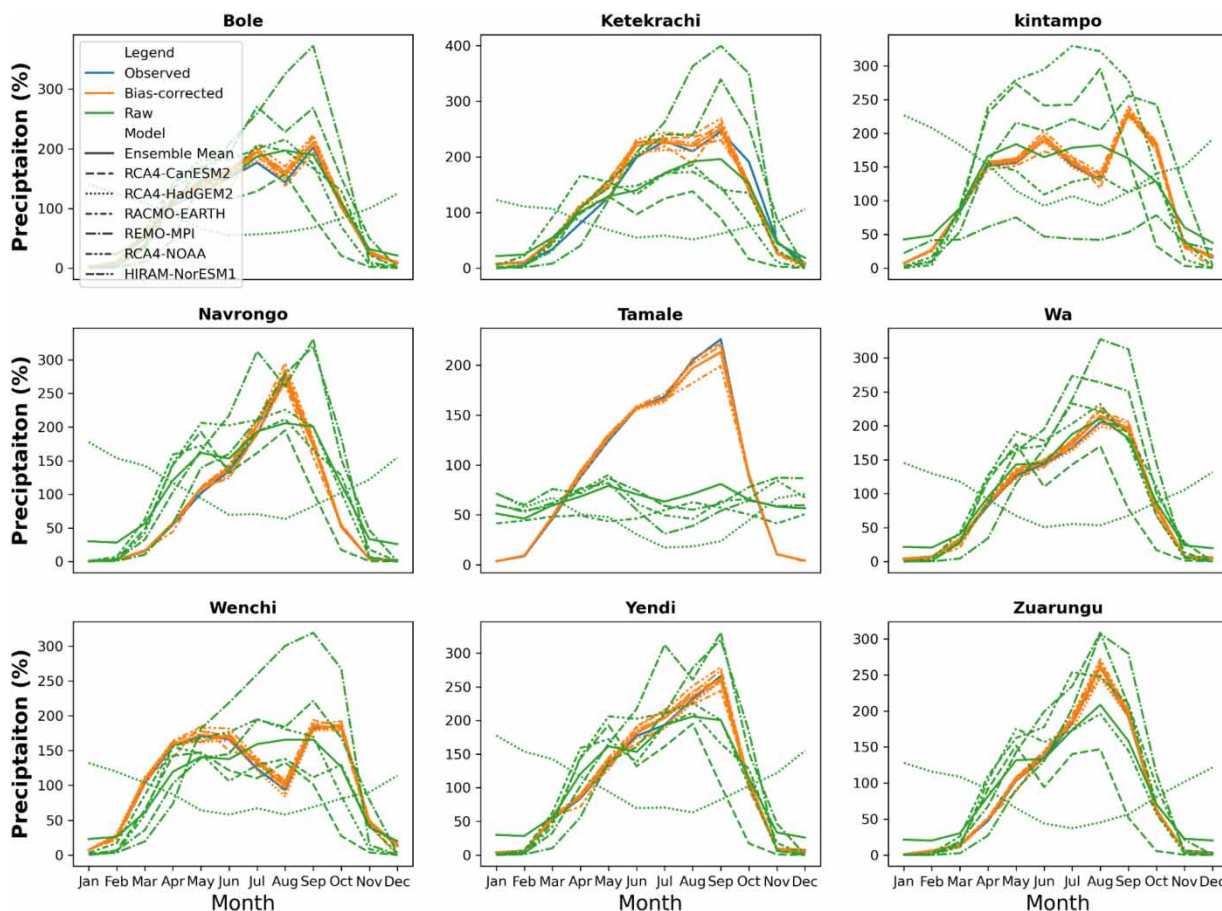


Figure 2 | Raw and bias-corrected simulations of observed monthly rainfall (1960–2005).

stations receive rainfall. This observation can be attributed to the reported challenges faced by RCMs in simulating the WAM, especially during the rainy season.

3.3. Model performance for annual temperature

The accuracy of RCMs in reproducing mean annual minimum temperature (T_{\min}) and maximum temperature (T_{\max}) was higher as compared to the simulation of rainfall (Figure 3). All other RCMs apart from RCA4-HadGEM2 were able to model the observed temperature (both T_{\min} and T_{\max}) with varying levels of accuracy. RAMO-EARTH was observed to underestimate both T_{\min} and T_{\max} at all locations consistently. At Tamale, none of the RCMs was able to model the observed pattern for both T_{\min} and T_{\max} .

Barring Tamale, the MAE and RMSE values for the raw RCMs for both T_{\min} and T_{\max} ranged from 1 to 4 °C (Table 3). Values recorded for both MAE and RMSE at Tamale were relatively high for all the RCMs and ranged from 15 to 18 °C and 16 to 20 °C, respectively. R^2 values recorded ranged from 0.2 to 0.98, except again for Tamale where values in the range of 0.04–0.4 were recorded for T_{\min} . Wenchi (T_{\max}) and Kete-Krachi (T_{\min} and T_{\max}) recorded some of the highest R^2 values (Table 3).

The ensemble means of the raw RCMs recorded MAE and RMSE values ranging from 1 to 2 °C for all stations for both T_{\min} and T_{\max} apart from Tamale that recorded MAE values of 15 and 16 °C for T_{\min} and T_{\max} , respectively, and RMSE values of 15 and 18 °C for T_{\min} and T_{\max} , respectively (Table 3).

R^2 values recorded for the ensemble mean were in the range of 0.04–0.98 (Table 3). The lowest value was recorded for T_{\min} at Tamale, while the highest was recorded at Wenchi for T_{\max} .

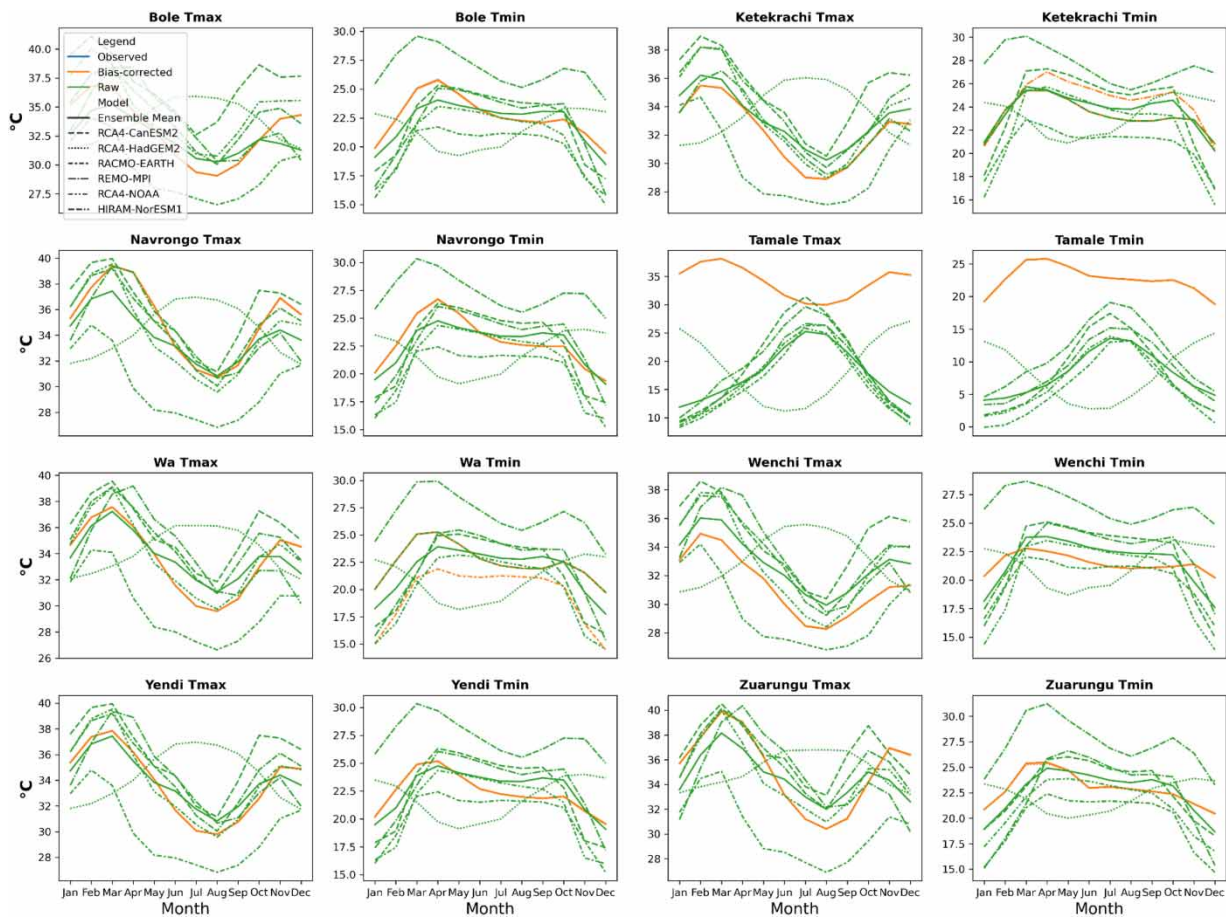


Figure 3 | Raw and bias-corrected simulations of observed temperature (T_{\max} and T_{\min}) from 1975 to 2005.

Similar to the observations made with precipitation, bias correction improved the ability of the RCMs in simulating the observed temperature. All the stations recorded MAE and RMSE values of 0 for all stations for both T_{\min} and T_{\max} . Since both the RMSE and MAE measure the degree of error between the observed and simulated data, it is accepted that the closer a value is to 0, the more similar the simulated value is to the observed. It indicates little or no residuals between the observed and simulated data. Thus, the MAE and RMSE values of 0 that were recorded indicate that after bias correction, the RCMs were able to simulate the observed data with a high level of performance. Also, each RCM recorded an R^2 value of 1 after bias correction for all stations. A further indication of the high performance of the RCMs in the stimulation of 1 implies that the simulated data are a perfect fit for the observed. The ensemble mean of the bias-corrected RCMs produced similar results to that of the individual RCMs. Zero was its value for both MAE and RMSE for all stations, as well as an R^2 value of 1.

3.4. Simulation of mean monthly T_{\min} and T_{\max}

Generally, T_{\min} was observed to be lowest in January and then gradually increased till it peaked in March/April. It then again declined from May till a second (smaller) peak was observed in October, after which it fell till December. For T_{\max} on the other hand, it was found to be high in January and continued to increase till it peaked in March/April and then declined sharply to its lowest in July/August, after which it increased again till December. These monthly T_{\min} and T_{\max} patterns were generally captured by the raw RCMs, albeit with varying levels of accuracy for each climate station (Figure 3). For T_{\min} , there were mixed simulations by the RCMs for the various locations. RACMO-EARTH, however, consistently underpredicted, while HIRAM-NorESM1 overpredicted for all stations. These observations are likely to be the result of the underlying boundary conditions used in the creation of these models.

On the other hand, for T_{\max} , almost all the months were slightly overpredicted for most stations by almost all raw RCMs, apart from Navrongo and Zuarungu where some underpredictions were observed. RACMO-EARTH again consistently underpredicted for T_{\max} for practically all stations and months. Tamale was the only station that recorded extreme values for both T_{\min} and T_{\max} by all RCMs.

For all the other stations (except Tamale), simulations overpredicted the observed temperature by as much as 7 °C, which was recorded at Wenchi for T_{\max} by RCA4-HadGEM2 for July and August. The highest underprediction was 9 °C, registered at Navrongo for T_{\max} for April by RACMO-EARTH. For Tamale, biases of both T_{\min} and T_{\max} were extremely high. All the RCMs underpredicted both T_{\min} and T_{\max} for all the months (Figure 3). The highest underprediction was recorded in March by a value of 24 °C for T_{\min} by RACMO-EARTH, while that of T_{\max} was 28 °C recorded in February by the same RCM (Figure 3).

After correction, the biases were almost completely removed, as mentioned in the previous section. All the bias-corrected RCMs were able to reproduce the same monthly means as observed at all the stations.

3.5. Projected changes in future climate

Based on the previous results, only the bias-corrected ensemble means were considered for analysis in this section. Future projections were analyzed for each station for the three epochs according to the World Meteorological Organisation (Ondras 2011; Gulacha & Mulungu 2016), with 30-year intervals, namely the 2020s (2006–2035), 2050s (2036–2065), and 2080s (2066–2095). These epochs were then used to undertake the change analysis in future climates. The future analysis was undertaken for both RCP 4.5 and RCP 8.5 using the baseline 1960–2005 and 1975–2005 for rainfall and temperature, respectively, and each RCM and then the ensemble mean. Change in rainfall was calculated as a percentage difference, while that of temperature was derived as the absolute difference. A positive signal was an indication of an increase in the variable (either rainfall or temperature), while a negative sign indicated a reduction with respect to the baseline period.

3.6. Projected monthly rainfall

Percentage differences in rainfall between the projected rainfall amounts and the baseline amount showed variations based on location and the period under consideration (Figure 4). The 2020s, for most sites, showed either declines or the least increase in rainfall amounts as compared to the other epochs.

3.7. Projected annual rainfall

The general projections under RCP 4.5 showed a decline in rainfall amounts for all three future epochs (Figure 5). The majority of the stations recorded the highest reductions in the 2020s except for Kete-Krachi where the least decline was recorded in the 2020s and for Bole where an increase was instead observed in the 2080s.

Projections under RCP 8.5, on the hand, showed variations with respect to locations. Stations such as Kete-Krachi and Zuarungu, as well as the entire study area, had simulations similar to those projected under RCP 4.5. All the other sites had projected declines in the 2020s and increases in either the 2050s or 2080s or both.

An exception to the aforementioned observation was noted at Tamale, where projections by both RCPs for three epochs showed declines that exceeded 60%.

3.8. Projected changes monthly temperature

Projected changes in monthly T_{\min} (Figure 6) showed that T_{\min} increased for all three epochs with the 2020s recording the least increase, while the 2080s marked the highest for both RCP 4.5 and RCP 8.5. Generally, the highest projected increases in T_{\min} were recorded in March and peaked in May, after which it declined for both RCP 4.5 and RCP 8.5. However, there were a few spikes observed in December and January for the 2050s and 2080s for both RCPs at some locations. As expected, the simulations by RCP 8.5 were generally higher than those under RCP 4.5 because of the conditions under which those scenarios were created.

Under RCP 4.5, the 2050s and 2080s recorded appreciations in all months at all locations. However, for the 2020s, some stations recorded reductions in T_{\min} for October, November, and January. Stations such as Bole, Navrongo, and Tamale recorded declines in all these months. At Kete-Krachi, declines were in November and January. At Wa, there was an increase in all the months, while Wenchi, on the other hand, recorded no change in T_{\min} for October and November but declines in December and January. Reductions were observed in September and October at Yendi, with no change occurring in August

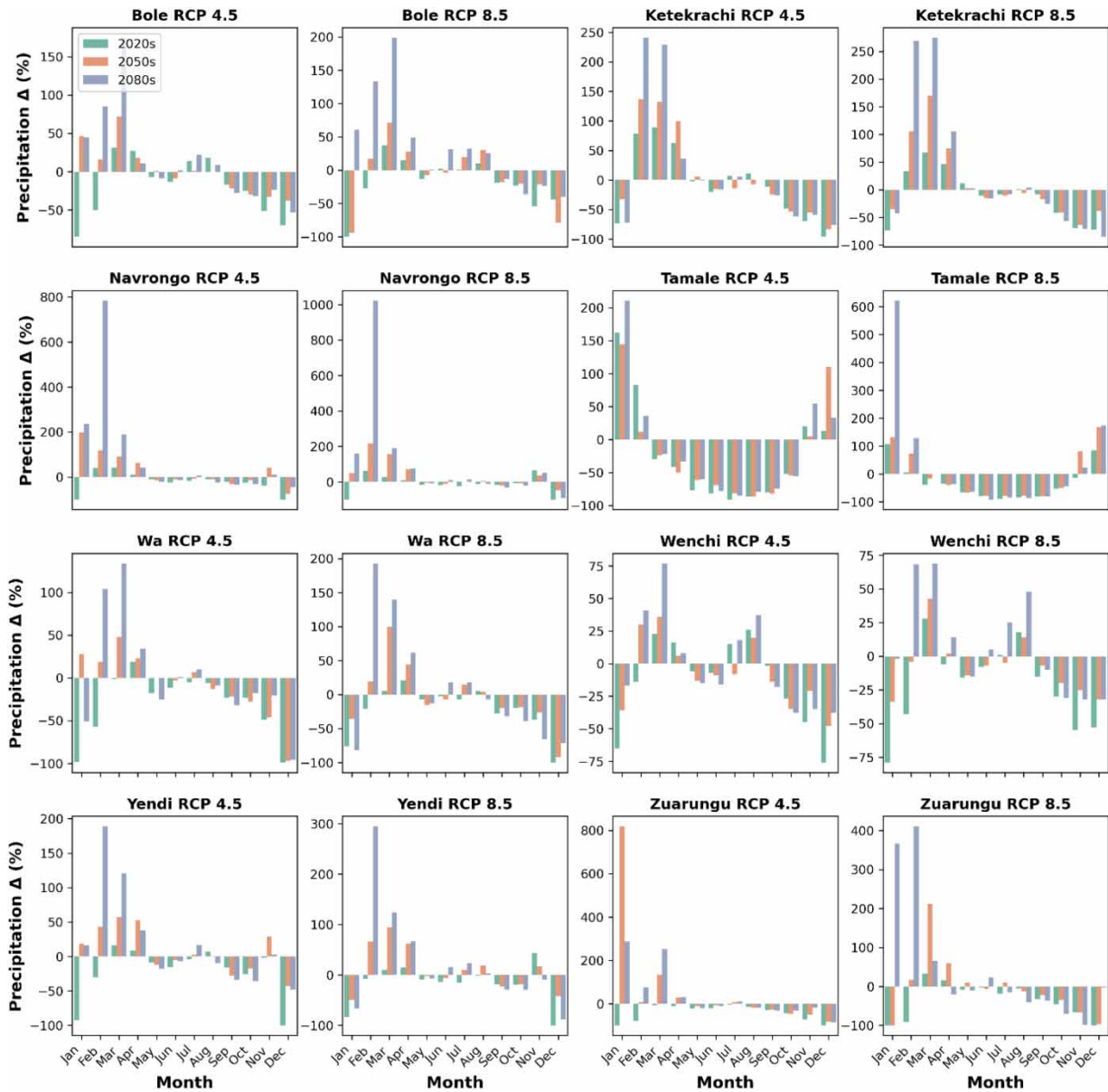


Figure 4 | Projected changes in monthly rainfall for the selected stations under RCP 4.5 and 8.5.

and November. Finally, at Zuarungu, all months recorded appreciations apart from November and December where no difference was observed.

Similar to the observations made under RCP 4.5, projections under RCP 8.5 showed that for locations such as Bole and Kete-Krachi, declines were noticed in November. Navrongo and Tamale recorded declines in November and December, while all months showed appreciations at Wa. At Wenchi, a decrease was seen in January, while no change occurred in October, November, and December. No change in T_{\min} was noticed in September and November, while a decline was recorded in October at Yendi. At Zuarungu, all months showed increases in T_{\min} apart from November when no change was recorded.

The simulated T_{\min} changes were about 1 or 2 °C for most months with a few of them recording no change (0 °C) for the 2020s. T_{\min} then increased from 2 to 6 °C in the 2050s and from 2 to 9 °C in the 2080s, with a few variations with the location.

Analogous to the projected changes in T_{\min} , the simulated T_{\max} changes were about 1 or 2 °C for most months with a few of them recording no change (0 °C) for the 2020s (Figure 6). It increased from 2 to 6 °C in the 2050s and from 2 to 9 °C in the 2080s, with a few variations with location.

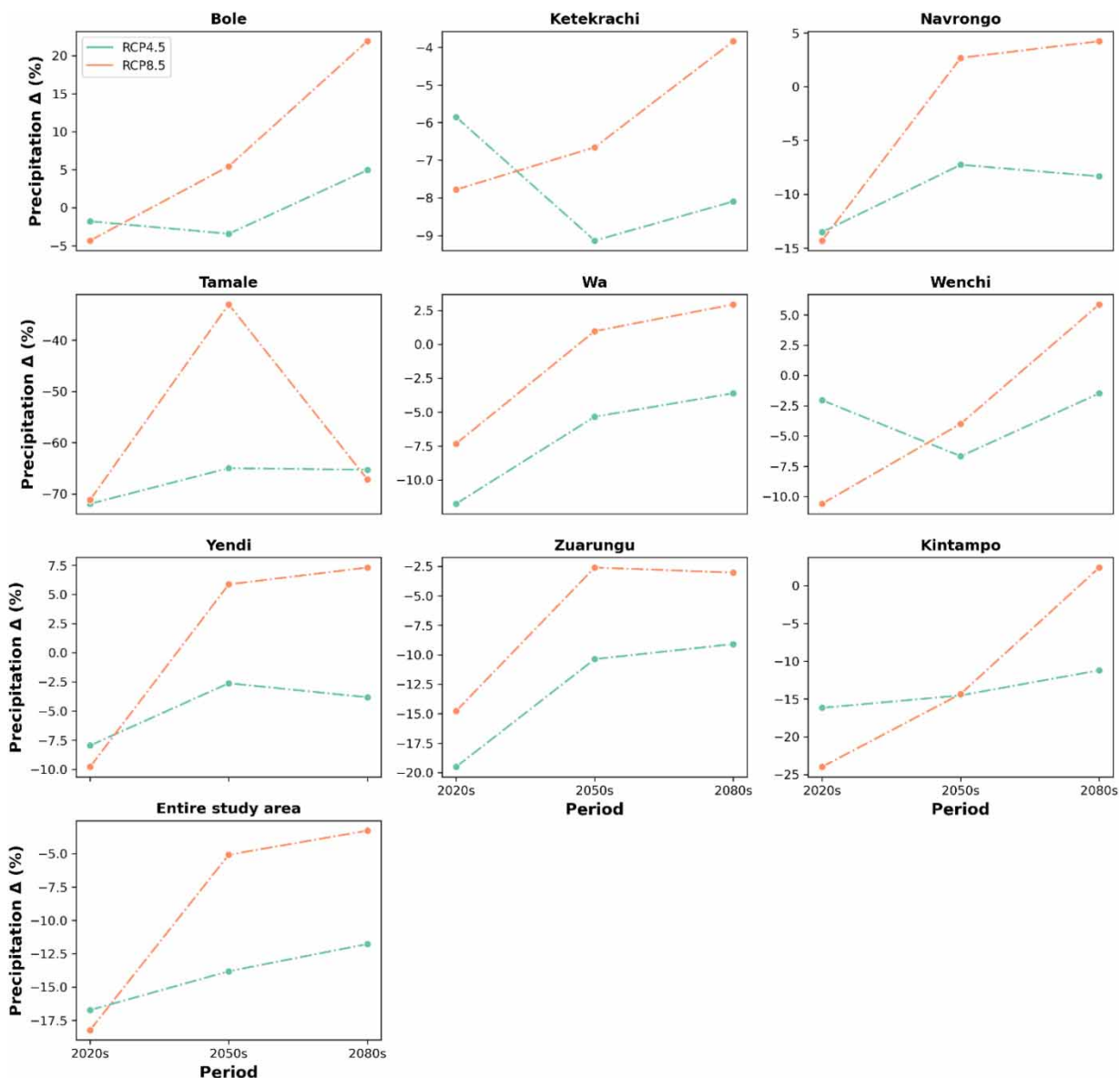


Figure 5 | Projected changes in annual rainfall under RCP 4.5 and 8.5.

The projected changes in T_{max} varied with location and epoch, under RCP 4.5 and RCP 8.5 (Figure 7). Stations such as Bole, Kete-Krachi, and Wenchi recorded increases in all the months for all periods except in the 2020s where no change was observed in June, July, August, and September. The situation at Navrongo and Zuarungu was similar to the above except that in their case, and September recorded an increase in T_{max} . At Tamale, no change in T_{max} was observed in January, February, and March for the 2020s, July and August for the 2050s, and December for the 2020s and 2080s. No change was also noticed for October and November for all three epochs. At Wa, all the months showed increases apart from February and November for the 2020s and March and April for all three periods. Finally, at Yendi, for the 2020s, no changes were noticed in February, May, and June, while declines were recorded in March and April. No changes in T_{max} were projected for March and April for the 2050s and 2080s.

Similar to the observations made under RCP 4.5, locations such as Bole and Kete-Krachi, Navrongo, and Wenchi recorded increases in all the months for all epochs except in the 2020s where no change was observed in June, July, August, and September (Figure 7). Again, at Tamale, no change in T_{max} was seen in January, February, March, and December for the 2020s

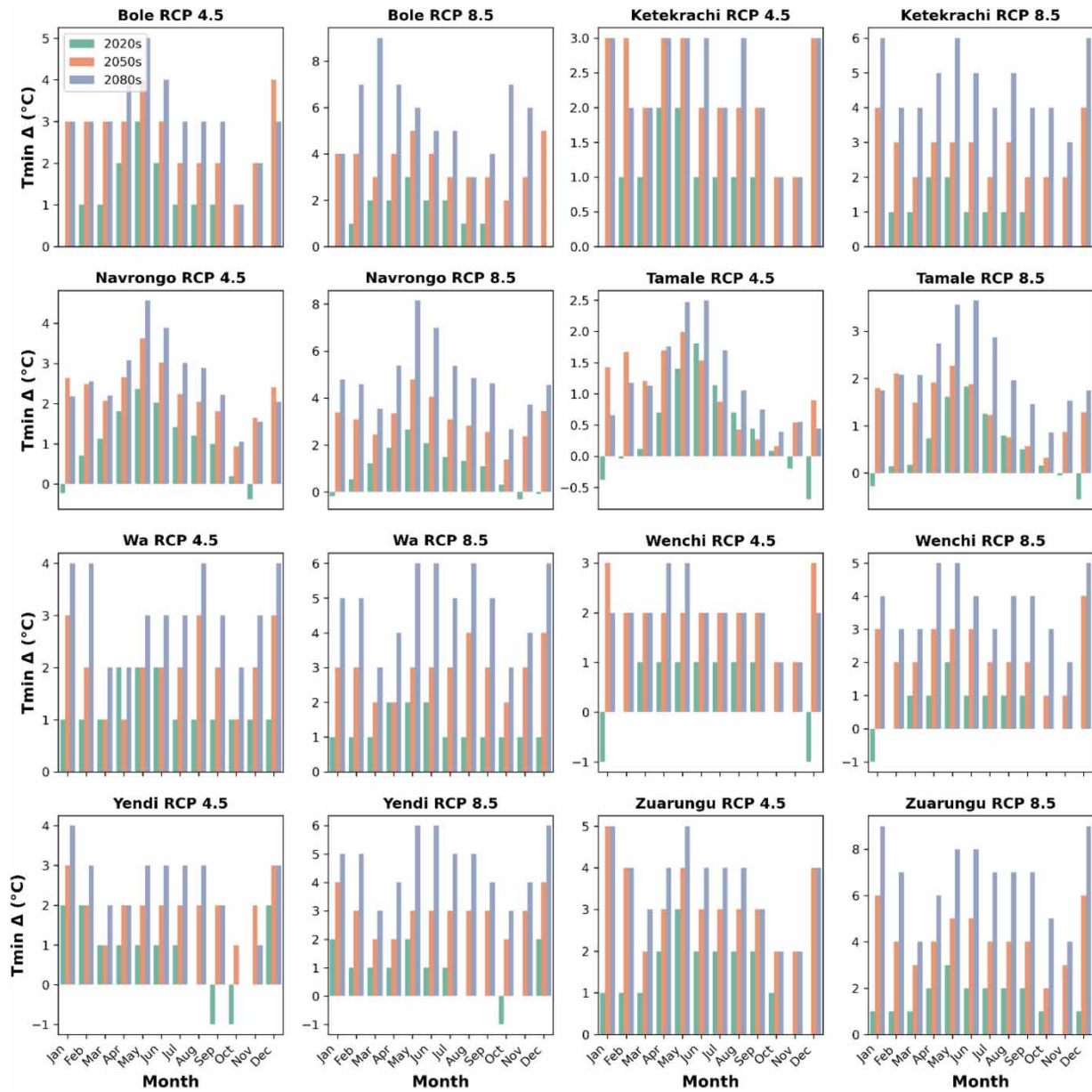


Figure 6 | Projected changes in monthly T_{min} for the selected stations under RCP 4.5 and 8.5.

and in October and November for both the 2020s and 2050s. At Wa, all the months showed appreciations apart from January, February, April, and November where no change was noticed for the 2020s and March, which recorded a decline. There was also no change projected for the 2050s for April. At Yendi, all months for all three epochs showed increasing T_{max} except March and April where T_{max} was projected to decline, and July for the 2020s where no change was recorded.

Generally, T_{max} is expected to increase in December, January, February, and March under the RCP 4.5 and RCP 8.5 across most of the stations (Figure 7). Comparably, T_{max} is expected to intensify under the worst-case scenario (RCP 8.5). For instance, T_{max} is expected to change by 6 °C at Yendi and Zuarungu under the RCP 8.5 (Figure 7).

3.9. Projected annual temperature

Projected changes in annual T_{min} as simulated for both RCP 4.5 and RCP 8.5 are presented in Figure 8. Apart from Bole where no change was recorded for the 2020s under RCP 8.5, all other locations recorded increased T_{min} for all future

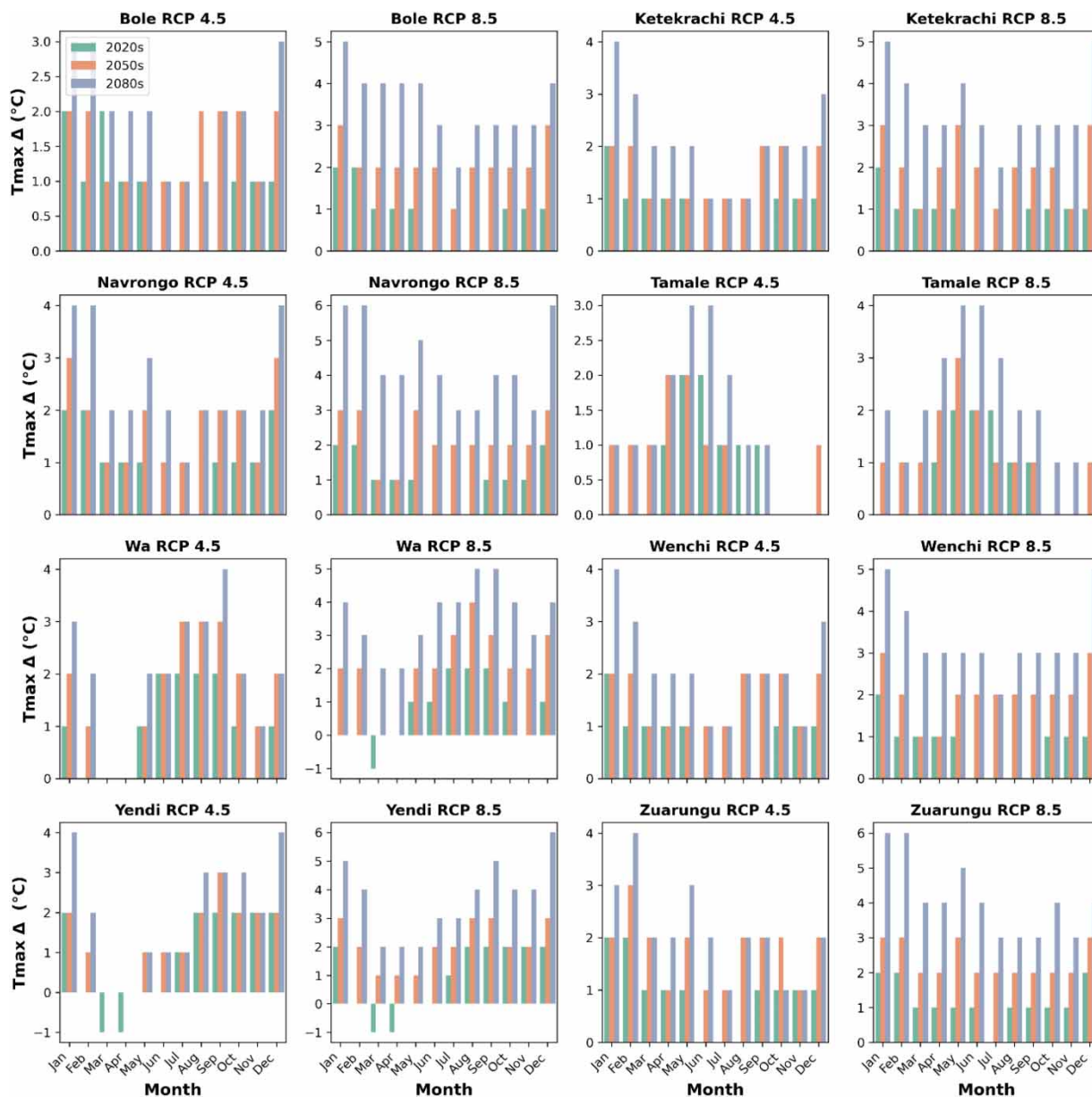


Figure 7 | Projected changes in monthly T_{max} for the selected stations under RCP 4.5 and 8.5.

epochs under both RCP 4.5 and RCP 8.5. A change of 1 °C was observed for both RCPs at all sites. For the 2050s, the changes ranged from 1 to 4 °C for both RCPs, 1 to 4 °C under RCP 4.5, and from 2 to 8 °C for the 2080s depending on the location

The most significant changes in the 2050s of 4 °C occurred at Bole and Zuarungu under RCP 4.5 and RCP 8.5, respectively.

For T_{max} under both RCP 4.5 and RCP 8.5, changes were relatively lower compared to the observations made for T_{min} (Figure 9). Similar to the pattern observed for T_{min} , the smallest changes were recorded in the 2020s and increased with progression from the 2050s to the 2080s barring Navrongo where a 2 °C change was observed in the 2020s. An increase of 1 °C was recorded at almost all locations except Navrongo for the 2020s, 1–2 °C for both the 2050s and 2080s under RCP 4.5.

For T_{max} , a 1 °C change was observed in the 2020s at all locations. For the 2050s, a 1 °C change was recorded at Tamale, while the rest of the stations recorded a 2 °C increase. For the 2080s, a T_{max} increase ranging from 1 to 4 °C was recorded.

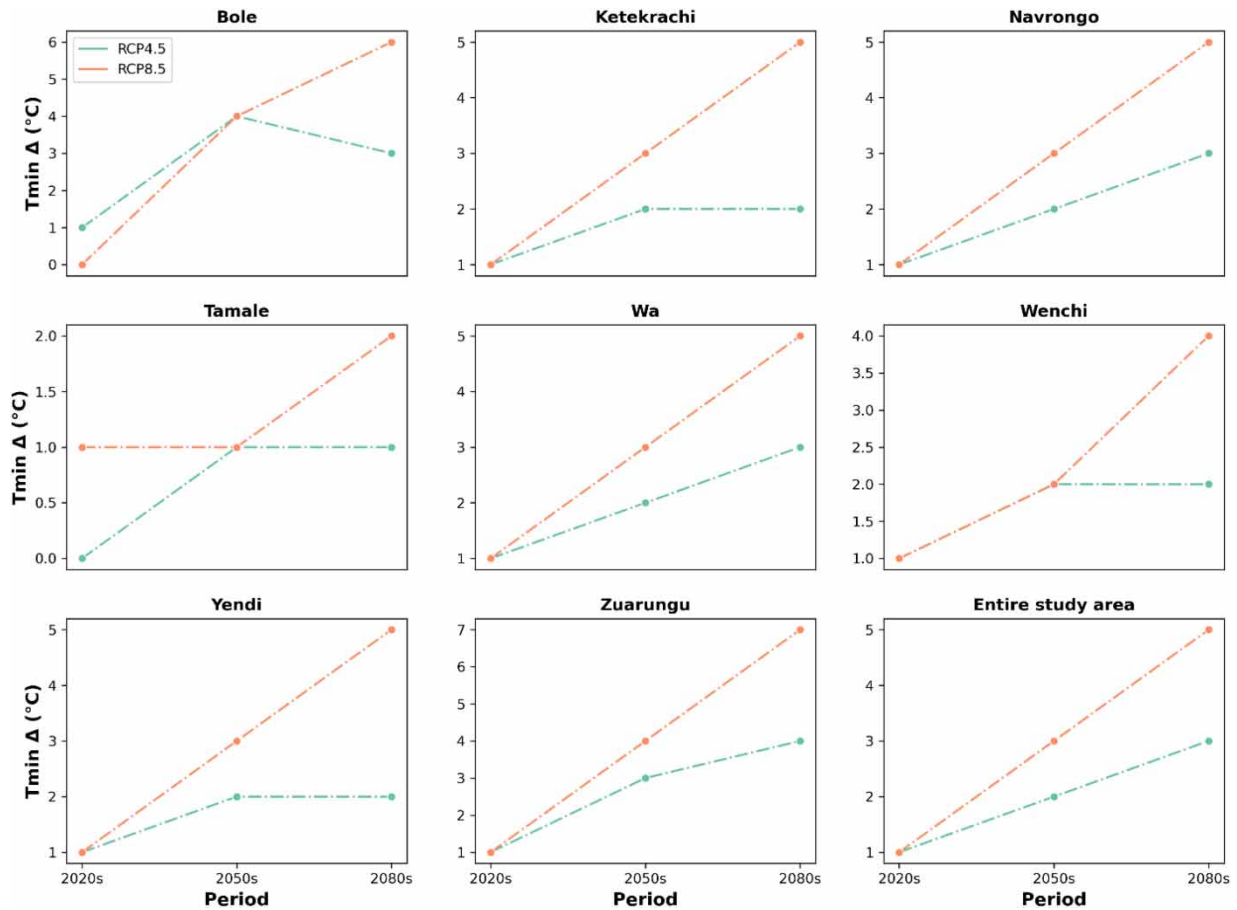


Figure 8 | Projected changes in annual T_{min} under RCP 4.5 and 8.5.

3.10. Projected change in mean annual temperature for the entire study area

The mean temperature changes projected for each climate station are presented in Figure 10. Under RCP 4.5, a 1 °C change was projected for all locations except Navrongo and Tamale where a mean temperature change of 1.5 and 0.5 °C was, respectively, recorded. For the 2050s, the projected changes ranged from 1.5 to 3 °C. However, no change was recorded at Tamale. For the 2080s, the change ranged from 2 to 4 °C.

Comparable to RCP 4.5, the projections under RCP 8.5 also showed a 1 °C change at all locations except Tamale where a mean temperature change of 0.5 °C was recorded. Projected changes ranged from 2 to 3 °C for the 2050s. For the 2080s, the change ranged from 2 to 5.5 °C (Figure 10).

4. DISCUSSION

In recent times, the West African subregion has experienced widespread reductions in rainfall amounts and increasing temperatures (Sylla & Nikiema 2016; Aziz & Obuobie 2017). However, the projection of precipitation in Africa and particularly West Africa comes with a high level of uncertainty and thus often presents no specific trend but with fluctuating amounts (IPCC 2013; Sylla & Nikiema 2016). The ability of RCMs to accurately project future climate depends largely on their ability to accurately reproduce past and present climate conditions. Therefore, evaluating the performance of RCMs in simulating such conditions is critical for climate change studies (Diallo *et al.* 2011; IPCC 2013; Sylla & Nikiema 2016). The ability of individual RCMs and their ensemble means to reproduce observed climate conditions have been varied depending on the climate variable and location. The differences in the RCM's ability to simulate the observed climate depend mostly on the driving model's representation of the WAM (Diallo *et al.* 2011; IPCC 2013; Sylla & Nikiema 2016).

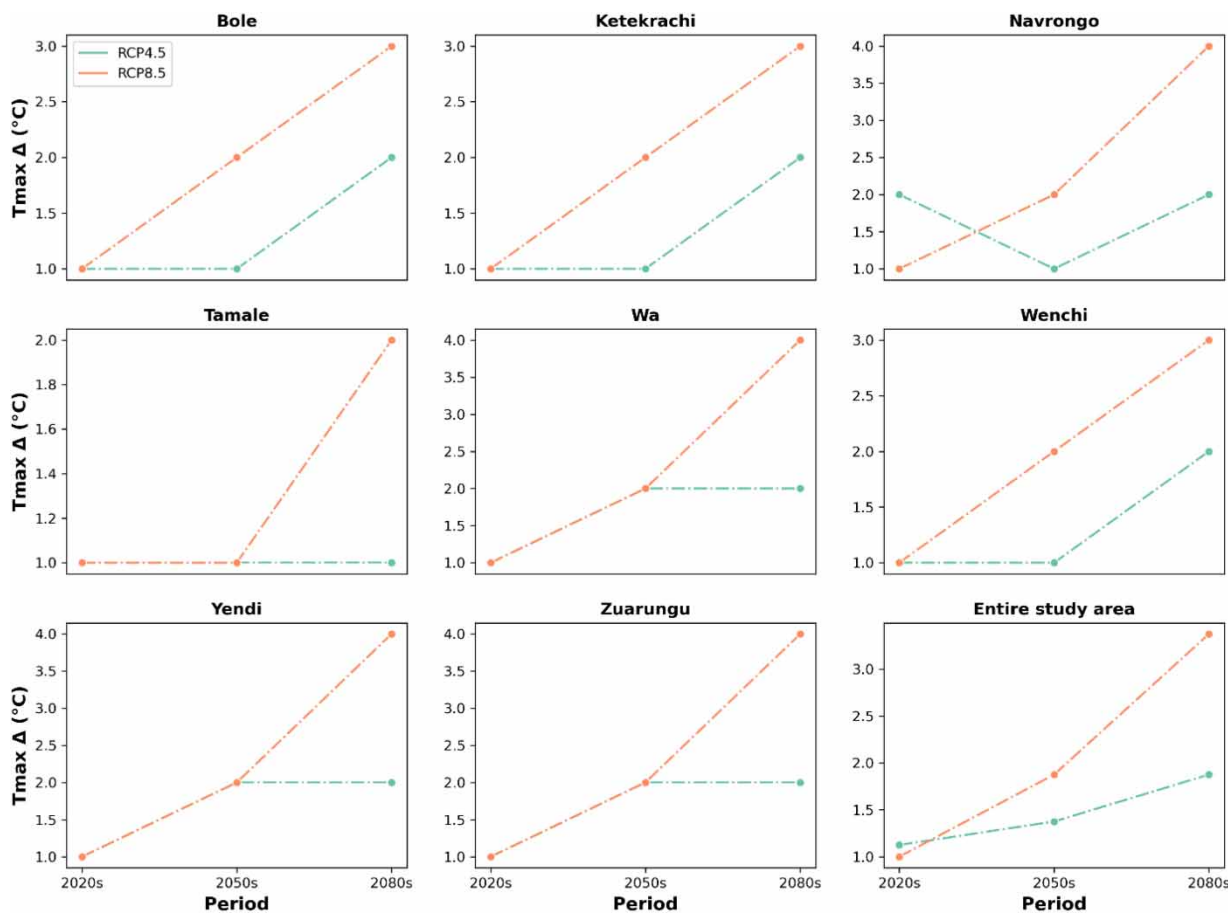


Figure 9 | Projected changes in annual T_{\max} under RCP 4.5 and 8.5.

In this study, RCMs generally performed better at simulating temperature than precipitation, even without bias correction. However, bias correction is mandatory for achieving higher accuracy as RCM data tends to deviate from observed data due to their inability to integrate all the chemical and physical processes in the atmosphere (Lupo & Kininmonth 2013; Lazoglou *et al.* 2019). This was evidenced by the fact that after bias correction, almost all RCMs satisfactorily simulated observed data and captured rainfall peaks unique to each climate station. A similar observation had also been reported by previous studies (Sylla & Nikiema 2016; Aziz & Obuobie 2017).

The ensemble mean was observed to outperform most of the individual RCMs in most cases both before and after bias correction. Although some studies have argued that in some cases, the ensemble mean is unable to outperform the individual RCMs or GCMs, a suitable RCM or GCM that is identified could be used instead. This observation holds for some locations (Tamale and Wa) where one or two individual RCMs were observed to outperform the ensemble mean. However, the margin of error in those instances for the ensemble mean was still within the acceptable range, and therefore, the ensemble mean could be employed for further analysis.

Overall, almost all climate stations showed projected increases in rainfall amounts, especially from January to March for the 2050s and 2080s, with declines observed from August to September, which is typically the peak of the rainy season. These changes may have significant implications for agriculture, as the declines coincide with the growing season and thus may potentially lead to crop failure.

Comparing projections under RCP 4.5 and RCP 8.5 showed a similar pattern, with variations in amounts. However, RCP 8.5 projections were generally higher due to the scenario's high emissions. The response of precipitation to increasing temperatures resulting from global warming has been reported to be far from homogenous, with oscillating values ranging from -30 to 30% (IPCC 2013; Sylla & Nikiema 2016). For this study, projected changes ranged from -20 to 20% for almost all locations, with the highest decline occurring in the 2020s under both RCP 4.5 and RCP 8.5, except for Tamale. This implies

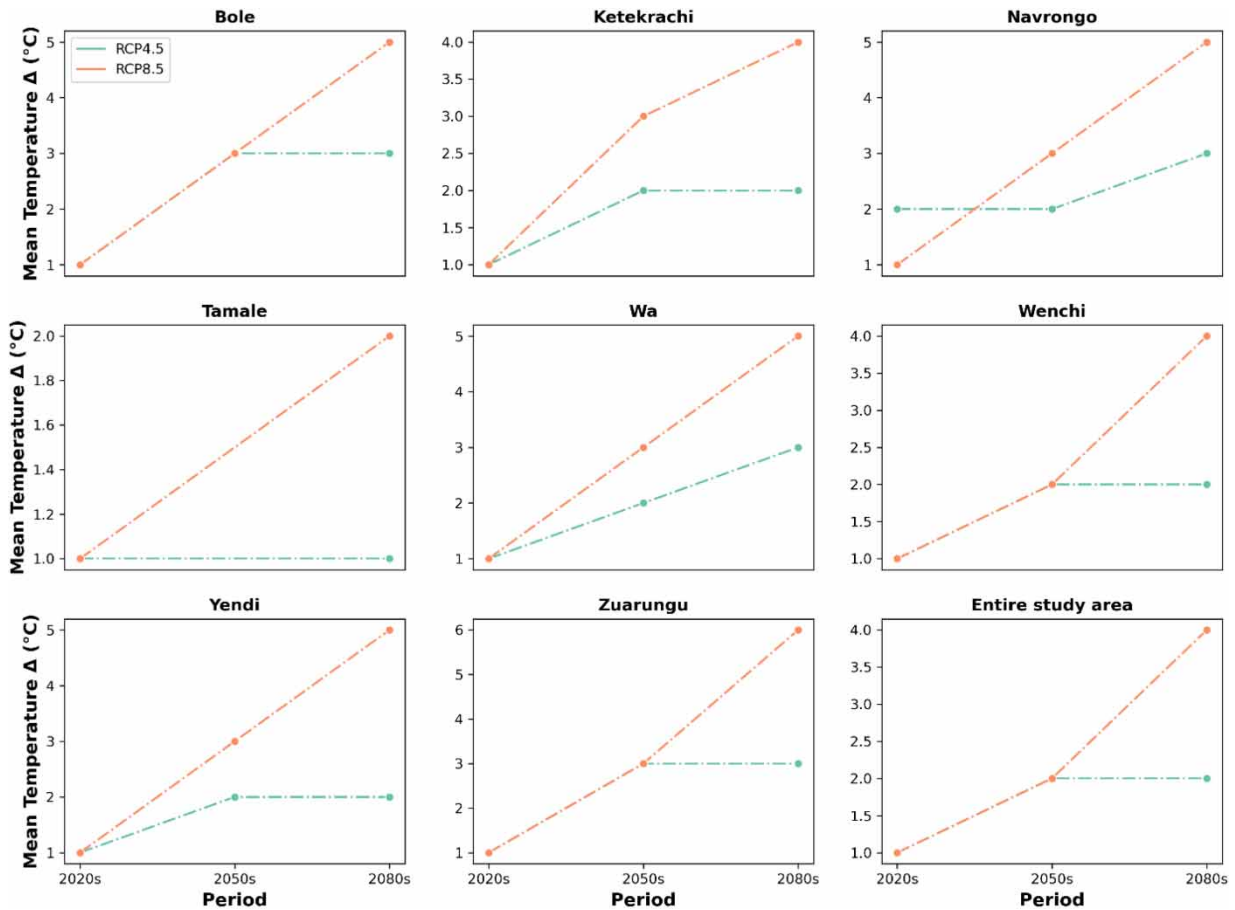


Figure 10 | Projected changes in mean temperature.

that projected changes are spatially variable, and therefore, there is the need for localized adaptation strategies to suit the need of the particular location.

A trend in extreme temperatures, particularly diurnal minimum, has been observed in West Africa during the second half of the 20th century (Mouhamed *et al.* 2013; Darko *et al.* 2018). Changes in T_{\min} were generally higher than T_{\max} , with T_{\min} being the temperature component most affected by slight changes in climate (Kim *et al.* 2013). The resultant effect could be a persistent warmer surface temperature since the cooling of the environment depends on the lower daily temperature. Similar projections for future temperature for the West African subregion had been made by Diallo *et al.* (2011) and Sylla & Nikiema (2016) and in the black Volta basin by Aziz & Obuobie (2017) in earlier studies suggesting that the entire region was undergoing warming.

A comparison of projected changes for the entire study area and individual locations produced varied results. Although they all projected temperature increases, the degree of change varied spatially. These variations ranged from about 1 to 3 °C, but for climate change studies, a 1 °C change in temperature is considered significant and could have dire consequences on the climate (IPCC 2013). It is thus critical to consider these variations in planning and executing adaptation strategies and policies to enhance sustainable agriculture and livelihoods.

However, more RCMs are needed to explore more possibilities regarding the uncertainty of RCM parameterization. Also, additional variables need to be examined (such as potential evapotranspiration and surface runoff) for gaining insight into the influence of climate change on the hydroclimate aspects of the Savannah regions.

5. CONCLUSION

The accuracy of both individual RCMs and their ensemble mean in simulating observed climate improved with bias correction. However, the performance of the raw ensemble mean was better than most of the raw individual RCMs in most cases.

The performance of individual RCMs varied with location. Noticeably, it was difficult for RCMs to simulate the climate pattern for Tamale for both rainfall and temperature. Although after bias correction, this situation was resolved, this challenge was again observed in the projection of future climate. These findings buttress previous studies that advocate for bias correction of RCMs before being used for further climate analysis. This is consistent with findings by Diallo *et al.* (2011), Gbobaniyi *et al.* (2014), and Nikulin *et al.* (2012). Again, the results also support those studies that have suggested the use of the multi-model ensemble mean of several RCMs instead of using just one, since the ensemble mean was found to outperform most of the individual RCMs for most locations (Teutschbein & Seibert 2010; Nikulin *et al.* 2012; Gbobaniyi *et al.* 2014). Although there were a few instances where a single RCM performed better than the ensemble mean, generally the ensemble mean was the best-performing model.

The overall changes in annual precipitation, as projected by the individual RCMs and their ensemble mean was a general decline in rainfall amounts, albeit with variations based on the RCM and location. As has been established by earlier studies, the changes in rainfall were found to be variable, oscillating between positive signals and negative signals with no particular trend. The change signal projected by the ensemble mean ranged from -20 to 20% for almost all locations, with the highest decline occurring in the 2020s. Some of the individual RCMs, however, projected change signals larger than these values. The 2050s recorded a relatively lower decline, while the 2080s generally recorded the smallest declines or in some cases increased. This observation was true for the analysis of the entire study area as well. In congruence with previous studies, simulations under RCP 8.5 were observed to be larger than the simulations under RCP 4.5.

The accuracy of simulating observed temperature by the individual RCMs improved with bias correction just as it did with rainfall, with the ensemble mean generally outperforming the individual RCMs in both cases.

The projected change in temperature showed an apparent increase in temperature over the study area for the various climate locations as well as for the entire study area. The mean temperature changes recorded were $1\text{ }^{\circ}\text{C}$ for the 2020s and $2\text{ }^{\circ}\text{C}$ for both the 2050s and the 2080s, in consonance with previous studies in the region as well as global predictions.

DATA AVAILABILITY STATEMENT

Data cannot be made publicly available; readers should contact the corresponding author for details.

CONFLICT OF INTEREST

The authors declare there is no conflict.

REFERENCES

- Afiesimama, E. A., Pal, J. S., Abiodun, B. J., Gutowski, W. J. & Adedoyin, A. 2006 Simulation of West African monsoon using the RegCM3. Part I: model validation and interannual variability. *Theoretical and Applied Climatology* **86** (1–4), 23–37. <https://doi.org/10.1007/s00704-005-0202-8>.
- Amirabadizadeh, M., Halim Ghazali, A., Huang, Y. F. & Wayayok, A. 2016 International journal of water resources and environmental engineering downscaling daily precipitation and temperatures over the Langat River Basin in Malaysia: a comparison of two statistical downscaling approaches. *Researchgate.Net* **8** (10), 120–136. <https://doi.org/10.5897/IJWREE2016.0585>.
- Awotwi, A., Annor, T., Anornu, G. K., Quaye-Ballard, J. A., Agyekum, J., Ampadu, B., Nti, I. K., Gyampo, M. A. & Boakye, E. 2021 Climate change impact on streamflow in a tropical basin of Ghana, West Africa. *Journal of Hydrology: Regional Studies* **34**, 100805.
- Aziz, F. & Obuobie, E. 2017 Trend analysis in observed and projected precipitation and mean temperature over the Black Volta Basin, West Africa. *International Journal of Current Engineering and Technology* **7** (4), 1400–1412.
- Bennett, N. D., Croke, B. F. W., Guariso, G., Guillaume, J. H. A., Hamilton, S. H., Jakeman, A. J., Marsili-Libelli, S., Newham, L. T. H., Norton, J. P., Perrin, C., Pierce, S. A., Robson, B., Seppelt, R., Voinov, A. A., Fath, B. D. & Andreassian, V. 2013 Characterising performance of environmental models. *Environmental Modelling and Software* **40**, 1–20. <https://doi.org/10.1016/j.envsoft.2012.09.011>.
- Boko, M., Niang, I., Nyong, A., Vogel, C., Githeko, A., Medany, M., Osman-Elasha, B., Tabo, R. & Yanda, P. 2008 Africa, climate change 2007: impacts, adaptation and vulnerability. Contribution of working group II to the fourth assessment report of the intergovernmental panel on climate change. In: *Climate Change 2007: Impacts, Adaptation and Vulnerability. Contribution of Working Group II to the Fourth Assessment Report of the Intergovernmental Panel on Climate Change*. pp. 433–467. <https://doi.org/10.2134/jeq2008.0015br>.
- Christensen, J. H., Hewitson, B., Busuioc, A., Chen, A., Gao, X., Held, I. & ... Whetton, P. 2007 Chapter 11: Regional climate projections.
- Christensen, J. H., Boberg, F., Christensen, O. B. & Lucas-Picher, P. 2008 On the need for bias correction of regional climate change projections of temperature and precipitation. *Geophysical Research Letters* **35** (20). <https://doi.org/10.1029/2008GL035694>.

- Darko, D., Adjei, K. A., Odai, S. N., Obuobie, E., Asmah, R. & Trolle, D. 2018 Recent climate trends for the Volta Basin in West Africa. *Weather*. <https://doi.org/10.1002/wea.3303>.
- Diallo, I., Sylla, M. B., Giorgi, F., Gaye, A. T. & Camara, M. 2011 Multimodel GCM-RCM ensemble-based projections of temperature and precipitation over West Africa for the early 21st century. *International Journal of Geophysics* **2012**. <https://doi.org/10.1155/2012/972896>.
- Faye, A. & Akinsola, A. A. 2021 Evaluation of extreme precipitation indices over West Africa in CMIP6 models. *Climate Dynamics*. <https://doi.org/10.1007/s00382-021-05942-2>.
- Foamouhoue, K. A. & Buscarlet, E. 2006 *Simulation du climat de l'Afrique de l'Ouest à l'aide d'un modèle climatique régional: Validation sur la période 1961–1990, documents.irevues.inist.fr*. Available from: www.cpc. (accessed 20 February 2020).
- Gbobaniyi, E., Sarr, A., Sylla, B., Diallo, I., Kamga, A., Browne, A., Dosio, A., Dhi, A., Hewitson, B. & Lamptey, B. 2014 Climatology, annual cycle and interannual variability of precipitation and temperature in CORDEX simulations over West Africa. **34**, 2241–2257. <https://doi.org/10.1002/joc.3834>.
- Ghansah, B., Forkuo, E. K., Osei, E. F., Appoh, R. K., Asare, M. Y. & Kluste, N. A. B. 2018 Mapping the spatial distribution of small reservoirs in the White Volta Sub-basin of Ghana. *Remote Sensing Applications: Society and Environment* **9**, 107–115. <https://doi.org/10.1016/j.rsase.2017.12.003>.
- Giménez, P. O. & García-Galiano, S. G. 2018 Assessing regional climate models (RCMs) ensemble-driven reference evapotranspiration over Spain. *Water (Switzerland)* **10** (9), 1–13. doi:10.3390/w10091181.
- Giorgi, F., Coppola, E., Solmon, F., Mariotti, L., Sylla, M. B., Bi, X. & Elguindi, N. 2012 RegCM4: model description and preliminary tests over multiple CORDEX domains. *Climate Research* **52**, 7–29. <https://doi.org/10.3354/cr01018>.
- Gulacha, M. M. & Mulungu, D. M. M. 2016 Generation of climate change scenarios for precipitation and temperature at local scales using SDSM in Wami-Ruvu River Basin, Tanzania. *Physics and Chemistry of the Earth*. <https://doi.org/10.1016/j.pce.2016.10.003>.
- Hourdin, F., Musat, I., Guichard, F., Ruti, P. M., Favot, F., Filiberti, M. A., Pham, M. A., Grandpeix, J. Y., Polcher, J. A. N., Marquet, P., Boone, A., Lafore, J. P., Redelsperger, J. L., Dell'Aquila, A., Doval, T. L., Traore, A. K. & Gallée, H. 2010 Amma-model intercomparison project. *Bulletin of the American Meteorological Society* **91** (1), 95–104. <https://doi.org/10.1175/2009BAMS2791.1>.
- Ibebuchie, C. C. 2021 On the representation of atmospheric circulation models in regional climate modes over Western Europe. *International Journal of Climatology* **3**, 668–682. <https://doi.org/10.1002/joc.7807>.
- Ibebuchie, C. C. 2022 Circulation type analysis of regional hydrology: the added value in using CMIP6 over CMIP5 simulations as exemplified from the MPI-ESM-LR model. *Journal of Water and Climate Change* **13** (2), 1046–1055. <https://doi.org/10.2166/wcc.2021.262>.
- Intergovernmental Panel on Climate Change (IPCC) 2001 The carbon cycle and atmospheric carbon dioxide. In: *Climate Change 2001: The Scientific Basis. Contribution of Working Group I to the Third Assessment Report of the Intergovernmental Panel on Climate Change*. <https://doi.org/10.1256/004316502320517344>.
- Intergovernmental Panel on Climate Change (IPCC) 2007 *Climate Change 2007: Impacts, Adaptation and Vulnerability: Contribution of Working Group II to the Fourth Assessment Report of the Intergovernmental Panel*. <https://doi.org/10.1256/004316502320517344>.
- Intergovernmental Panel on Climate Change (IPCC) 2013 Summary for policymakers. *Climate Change 2013: The Physical Science Basis Contribution of Working Group I to the Fifth Assessment Report of the Intergovernmental Panel on Climate Change*.
- Islam, M. N. 2008 *Analysis and Modelling of Climate Change*. pp. 61–66.
- Johnson, F. & Sharma, A. 2015 What are the impacts of bias correction on future drought projections? *Journal of Hydrology* **525**, 472–485. <https://doi.org/10.1016/j.jhydrol.2015.04.002>.
- Kalognomou, E. A., Lennard, C., Shongwe, M., Pinto, I., Favre, A., Kent, M. & ... Büchner, M. 2013 A diagnostic evaluation of precipitation in CORDEX models over Southern Africa. *Journal of Climate* **26** (23), 9477–9506. doi:10.1175/JCLI-D-12-00703.1.
- Kendon, E. J., Jones, R. G., Kjellstrom, E. & Murphy, J. M. 2010 Using and designing GCM – RCM ensemble regional climate projections. *Journal of Climate* **23**, 6485–6503. <https://doi.org/10.1175/2010JCLI3502.1>.
- Kim, J., Waliser, D. E., Mattmann, C. A., Goodale, C. E., Hart, A. F., Zimdars, P. A., Crichton, D. J., Jones, C., Nikulin, G., Hewitson, B., Jack, C., Lennard, C. & Favre, A. 2013 Evaluation of the CORDEX-Africa multi-RCM hindcast: systematic model errors. *Climate Dynamics* **42** (5–6), 1189–1202. <https://doi.org/10.1007/s00382-013-1751-7>.
- Kranjac-Berisavljevic, G., Bayorbor, T. B., Abdulai, A. S., Obeng, F., Blench, R. M., Turton, C. N. & ... Drake, E. 1999 *Rethinking Natural Resource Degradation in Semi-Arid Sub-Saharan Africa: The Case of Semi-Arid Ghana*. University for Development Studies, Tamale and ODI, London.
- Laprise, R., Hernández-Díaz, L., Tete, K., Sushama, L., Šeparović, L., Martynov, A., Winger, K. & Valin, M. 2013 Climate projections over CORDEX Africa domain using the fifth-generation Canadian Regional Climate Model (CRCM5). *Climate Dynamics* **41** (11–12), 3219–3246. <https://doi.org/10.1007/s00382-012-1651-2>.
- Lazoglou, G., Anagnostopoulou, C., Skoulikaris, C. & Tolika, K. 2019 Bias correction of climate model's precipitation using the copula method and its application in River Basin simulation. *Water (Switzerland)* **11** (5). <https://doi.org/10.3390/w11030600>.
- Liebe, J. R., Van De Giesen, N., Andreini, M., Walter, M. T. & Steenhuis, T. S. 2009 Determining watershed response in data poor environments with remotely sensed small reservoirs as runoff gauges. *Water Resources Research* **45** (7), 1–12. <https://doi.org/10.1029/2008WR007369>.

- Lupo, A. & Kininmonth, W. 2013 Global climate models and their limitations. *Nature Communications* **4** (1), 1764. <https://doi.org/10.1038/ncomms2656>.
- Moss, R. H., Edmonds, J. A., Hibbard, K. A., Manning, M. R., Rose, S. K., Van Vuuren, D. P., Carter, T. R., Emori, S., Kainuma, M., Kram, T., Meehl, G. A., Mitchell, J. F. B., Nakicenovic, N., Riahi, K., Smith, S. J., Stouffer, R. J., Thomson, A. M., Weyant, J. P. & Wilbanks, T. J. 2010 The next generation of scenarios for climate change research and assessment. *Nature* **463** (7282), 747–756. <https://doi.org/10.1038/nature08823>.
- Mouhamed, L., Traore, S. B., Alhassane, A. & Sarr, B. 2013 Evolution of some observed climate extremes in the West African Sahel. *Weather and Climate Extremes* **1**, 19–25. <https://doi.org/10.1016/j.wace.2013.07.005>.
- Nikulin, G., Jones, C., Giorgi, F., Asrar, G., Buchner, M., Cerezo-Mota, R., Christensen, O. B., Deque, M., Fernandez, J., Hansler, A., Van Meijgaard, E., Samuelson, P., Sylla, M. B. & Sushama, L. 2012 Precipitation climatology in an ensemble of CORDEX-Africa regional climate simulations. *Journal of Climate* **25**, 6057–6078. <https://doi.org/10.1175/JCLI-D-11-00375.1>.
- Obuobie, E. 2008 Estimation of groundwater recharge in the context of future climate change in the White Volta River Basin. *Ecology Series* **153**.
- Ondras, M. 2011 World Meteorological Organisation Standards and Best Practices.
- Paeth, H., Hall, N. M. J., Gaertner, M. A., Alonso, M. D., Moumouni, S., Polcher, J., Ruti, P. M., Fink, A. H., Gosset, M., Lebel, T., Gaye, A. T., Rowell, D. P., Moufouma-Okia, W., Jacob, D., Rockel, B., Giorgi, F. & Rummukainen, M. 2011 Progress in regional downscaling of West African precipitation. *Atmospheric Science Letters* **12** (1), 75–82. <https://doi.org/10.1002/asl.306>.
- Pal, J. S., Giorgi, F., Bi, X., Elguindi, N., Solmon, F., Gao, X., Rauscher, S. A., Francisco, R., Zakey, A., Winter, J., Ashfaq, M., Syed, F. S., Bell, J. L., Differbaugh, N. S., Karmacharya, J., Konari, A., Martinez, D., Da Rocha, R. P., Sloan, L. C. & Steiner, A. L. 2007 Regional climate modeling for the developing world: the ICTP RegCM3 and RegCM3. *Bulletin of the American Meteorological Society* **88** (9), 1395–1409. <https://doi.org/10.1175/BAMS-88-9-1395>.
- Rajib, M. A. & Rahman, M. 2012 A comprehensive modeling study on regional climate model (RCM) application – regional warming projections in monthly resolutions under IPCC A1B scenario. *Atmosphere*, 557–572. <https://doi.org/10.3390/atmos3040557>.
- Rathjens, H., Bieger, K., Srinivasan, R. & Arnold, J. G. 2016 CMhyd User Manual Documentation for Preparing Simulated Climate Change Data for Hydrologic Impact Studies.
- Safari, B., Sebaziga, J. N. & Siebert, A. 2021 Evaluating CORDEX-CORE regional climate models in simulating rainfall variability in Rwanda. *International Journal of Climatology* **43** (3). <https://doi.org/10.1002/joc.7891>.
- Santhi, C., Arnold, J. G., Williams, J. R., Dugas, W. A., Srinivasan, R. & Hauck, L. M. 2001 Validation of the SWAT model on a large river basin with point and nonpoint sources. *Journal of the American Water Resources Association* **37** (5), 1169–1188. <https://doi.org/10.1111/j.1752-1688.2001.tb03630.x>.
- Sennikovs, J. & Bethers, U. 2009 Statistical downscaling method of regional climate model results for hydrological modelling. In: *18th World IMACS/MODSIM Congress*. Available from: <http://mssanz.org.au/modsim09> (accessed 20 February 2020).
- Solman, S. A., Sanchez, E., Samuelsson, P., da Rocha, R. P., Li, L., Marengo, J., Pessacq, N. L., Remedio, A. R. C., Chou, S. C., Berbery, H., Le Treut, H., de Castro, M. & Jacob, D. 2015 Evaluation of an ensemble of regional climate model simulations over South America driven by the ERA-interim reanalysis: model performance and uncertainties. *Climate Dynamics* **41** (5–6), 1139–1157. <https://doi.org/10.1007/s00382-013-1667-2>.
- Sylla, M. B., Nikiema, P. M., 2016 Climate change over West Africa : recent trends and future projections. In: *Adaptation to Climate Change and Variability in Rural West Africa* (Yaro, J. A. & Hesselberg, J., eds). <https://doi.org/10.1007/978-3-319-31499-0>.
- Sylla, M. B., Gaye, A., Pal, J. S., Jenkins, G. & Bi, X. Q. 2009 High-resolution simulations of West African climate using regional climate model (RegCM3) with different lateral boundary conditions. *Theoretical and Applied Climatology* **98** (3–4), 293–314. <https://doi.org/10.1007/s00704-009-0110-4>.
- Teutschbein, C. & Seibert, J. 2010 Regional climate models for hydrological impact studies at the catchment scale: a review of recent modeling strategies: regional climate models for hydrological impact studies. *Geography Compass* **7**, 834–860. <https://doi.org/10.1111/j.1749-8198.2010.00357.x>.
- Teutschbein, C. & Seibert, J. 2012 Bias correction of regional climate model simulations for hydrological climate-change impact studies: review and evaluation of different methods. *Journal of Hydrology* **456–457**, 12–29. <https://doi.org/10.1016/j.jhydrol.2012.05.052>.
- Teutschbein, C. & Seibert, J. 2013 Is bias correction of regional climate model (RCM) simulations possible for non-stationary conditions. *Hydrology and Earth System Sciences* **17** (12), 5061–5077. <https://doi.org/10.5194/Hess-17-5061-2013>.
- Thornton, P. K., Ericksen, P. J., Herrero, M. & Challinor, A. J. 2014 Climate variability and vulnerability to climate change: a review. *Global Change Biology* **20** (11), 3313–3328. <https://doi.org/10.1111/gcb.12581>.
- Van Liew, M. W., Arnold, J. G. & Garbrecht, J. D. 2003 Hydrologic simulation on agricultural watersheds: choosing between two models. *Transactions of the American Society of Agricultural Engineers* **46** (6), 1539–1551. doi:10.13031/2013.15643.
- van Vuuren, D. P., Edmonds, J., Kainuma, M., Riahi, K., Thomson, A., Hibbard, K., Hurtt, G. C., Kram, T., Krey, V., Lamarque, J. F., Masui, T., Meinshausen, M., Nakicenovic, N., Smith, S. J. & Rose, S. K. 2011 The representative concentration pathways: an overview. *Climatic Change* **109** (1), 5–31. <https://doi.org/10.1007/s10584-011-0148-z>.
- Xue, Y., e Sales, F., Lau, W. K. M., Boone, A., Feng, J., Dirmeyer, P., Guo, Z., Kim, K. M., Kitoh, A., Kumar, V., Pocard-Leclercq, I., Mahowald, N., Moufouma-Okia, W., Pegion, P., Rowell, D. P., Schemm, J., Schubert, S. D., Sealy, A., Thiaw, W. M. & ... Wu, M. L. C. 2010 Intercomparison and analyses of the climatology of the West African Monsoon in the West African Monsoon Modeling and

Evaluation project (WAMME) first model intercomparison experiment. *Climate Dynamics* 35 (1), 3–27. <https://doi.org/10.1007/s00382-010-0778-2>.

Yira, Y., Diekkrüger, B., Steup, G. & Bossa, A. Y. 2017 Impact of climate change on hydrological conditions in a tropical West African catchment using an ensemble of climate simulations. 2143–2161. <https://doi.org/10.5194/hess-21-2143-2017>.

First received 14 February 2023; accepted in revised form 4 June 2023. Available online 17 June 2023